10-31-2005

Bulk Silicon Based Temperature Sensor

Bharath Bethala Kishanlal Premchand
University of South Florida

Bulk Silicon Based Temperature Sensor

by

Bharath Bethala Kishanlal Premchand

A thesis submitted in partial fulfillment
of the requirements for the degree of
Master of Science in Electrical Engineering
Department of Electrical Engineering
College of Engineering
University of South Florida

Major Professor: Shekhar Bhansali, Ph.D.
Larry Langebrake, P.E.
Kenneth Buckle, Ph.D.
Sang Chae Kim, Ph.D.

Date of Approval:
October 31, 2005

Keywords: transition elements, gold, diffusion, resistivity, resistance

DEDICATION

To my family

ACKNOWLEDGEMENTS

I am deeply grateful to Dr. Shekhar Bhansali for providing me the opportunity to pursue this research. I would also like to thank Larry Langebrake, Dr. Kenneth Buckle and Dr. Sang Chae Kim for agreeing to serve on my thesis committee.

Special thanks to Dr. Senthil Sambandam, Shyam Aravamudhan, Kevin Luongo Praveen Sekhar, and the members of Bio-MEMS and Microsystems lab at USF Tampa for their help.

I would also like to thank my friends for their support during this work. Finally, I would like to thank my family to whom I am, and will be indebted throughout my life for all their love and encouragement that has made this possible.

TABLE OF CONTENTS

LIST OF TABLES

LIST OF FIGURES

BULK SILICON BASED TEMPERATURE SENSOR

Bharath Bethala Kishanlal Premchand

ABSTRACT

A bulk silicon temperature sensor is fabricated in this work. The objective is to develop a low-cost high resolution temperature sensor. The target applications are a Conductivity-Temperature-Depth (CTD) sensor for oceanic applications and a magnetocaloric microcooler.

The properties of silicon are modified by thermal diffusion of gold. Gold is a fast diffuser in silicon and its diffusion contributes to the increase in resistivity of silicon. The addition of gold to n-type silicon creates a negative temperature coefficient device. The effect of the diffusing environment was investigated by diffusing in oxygen and nitrogen ambient at various temperatures. The influence of area of gold diffusion was also investigated. The effect of temperature on resistance was measured and was used to calibrate the sensor.

Although the sensors fabricated in an oxygen environment have an exponential type response, they can be used in the CTD application because of enhanced sensitivity in the 10˚C - 30˚C temperature range. Sensors fabricated in a nitrogen environment are found to have linear response with sensitivity ranging from 7Ω/˚C to 3000Ω/˚C and can be used for both applications. The fabricated sensors have a 0.1˚C resolution.

CHAPTER 1

INTRODUCTION

Mankind has always been inquisitive about its surroundings and this has been one of the main reasons it has reached where it is today. It is always the questions asked that have led to answers, some right and some to different questions.

1.1 Need for sensors

To understand the surroundings, it is necessary to measure phenomena like temperature, light and wind. The first sensors that primitive man used were the five senses of the human body namely sight, hearing, smell, taste and touch. As he evolved the development of instruments/devices took place to monitor phenomena to give more accurate readings and hence a better understanding. Ironically the modern man is still trying to replicate the human senses.

1.2 Importance of temperature sensing

Temperature is by far the most measured parameter in most experiments. It impacts biological, physical and chemical phenomena in numerous ways. Temperature plays an important part in determining the conditions in which living matter can exist. Birds and mammals demand a very narrow range of body temperatures for survival and

must be protected against extreme heat or cold. Aquatic species can exist only within a narrow temperature range of water, which differs for various species. Temperature changes the physical properties of materials. Materials generally expand/contract when subjected to a temperature change and this causes a variety of problems from space constraints in the case of rail tracks to measurement errors in the case of devices. Temperature affects the rate of a chemical reaction. Increasing the temperature generally increases the reaction rate by giving energy to the involved molecules/atoms.

Temperature measurement is required in a multitude of applications, varying from control of industrial processes, laboratory experiments, environmental control and biomedical instrumentation where knowing and using the actual or relative temperature is critical. For instance, other sensors such as pressure, force, flow, level, and position many times require temperature monitoring in order to insure accuracy.

1.3 Motivation

This work focuses on development and fabrication of a bulk silicon based temperature sensor. The main applications are a conductivity-temperature-depth (CTD) sensor and a magnetocaloric cooler.

The mean temperature of ocean has changed by 10˚C over the past 65 million years. Such large changes in temperature impact the biochemical cycling in the ocean and atmosphere. CTD sensors are used for oceanographic measurements and hence require a sensitive and robust temperature sensor to withstand harsh environments. The current state-of-art CTD sensors are about a meter long and $1/3^{rd}$ meter in diameter [1]. Also they are typically costly with a starting price of about $2000.

One of the primary goals of this research is to investigate and develop a silicon based sensor that can be integrated in a Micro-Electro-Mechanical-System (MEMS) based CTD sensor with obvious benefits of cost and size [2]. The other advantage of using MEMS based sensors are easy realization of a distributed network to get more accurate data.

The other application where the sensor will be implemented is magnetocaloric coolers which are being actively researched. They have the advantages of being environmental friendly and are capable of high efficiency as they can be designed without moving parts. In these coolers a magnetocaloric material undergoes an entropy change in varying magnetic fields, which is used for cooling purposes. The miniature magnetocaloric cooler requires in-situ temperature sensors to measure the temperature of liquid and hence the cooling efficiency [3]. The cooler is fabricated using micromachining technology in silicon. It would be easier to integrate a silicon based sensor in such a cooler.

The microsensor being investigated in this work is a bulk silicon based temperature sensor. It is fabricated by altering the properties of silicon through diffusion. Gold is diffused into silicon at high temperature. This affects the resistivity and temperature coefficient of resistance (TCR) of silicon significantly, making the electrical properties of silicon more sensitive to temperature. The fabrication parameters can be changed to develop temperature sensors that can be used for both applications mentioned above.

1.4 Thesis overview

In chapter 2 the classification of temperature sensors is presented. Various temperature sensors with their sensing ranges, advantages and drawbacks are discussed. Chapter 3 presents the theory and working of the temperature sensor. The effect of gold diffusion on silicon is discussed. In chapter 4 the fabrication of the sensor is shown. The measurement setups are also presented in detail. The results of the temperature sensors are presented in chapter 5. In chapter 6 the conclusions and future work are discussed. Chapter 6 also discusses incorporation of the sensor for the required applications.

CHAPTER 2

LITERATURE REVIEW

2.1 History of temperature sensing

Intuitively man has known about temperature for a long time. Galileo invented the first documented thermometer in about 1592. The thermometer was sensitive but was affected by atmospheric pressure. In 1714, Daniel Gabriel Fahrenheit invented both the mercury thermometer and the alcohol thermometer. At the time, thermometers were calibrated between the freezing point of salted water and the human body temperature [4].

The early 1800's were very productive in the area of temperature measurement and understanding. William Thompson (Lord Kelvin) postulated the existence of an absolute zero. In 1821 T. J. Seebeck discovered that a current could be produced by unequally heating two junctions of two dissimilar metals, the thermocouple effect. Also in 1821, Sir Humphrey Davy discovered that all metals have a positive TCR and that platinum could be used as an excellent temperature detector (RTD). These two discoveries marked the beginning of serious electrical sensors. The late 19^{th} century saw the introduction of bimetallic temperature sensor. These thermometers contain no liquid but operate on the principle of unequal expansion between two metals. The 20th century

has seen the discovery of semiconductor devices, such as: the thermistor, the integrated circuit sensor, a range of non-contact sensors and also fiber-optic temperature sensors.

2.2 Classification of temperature sensors

Temperature sensors can be grouped based on the temperature range of application as shown in Figure 2.1.

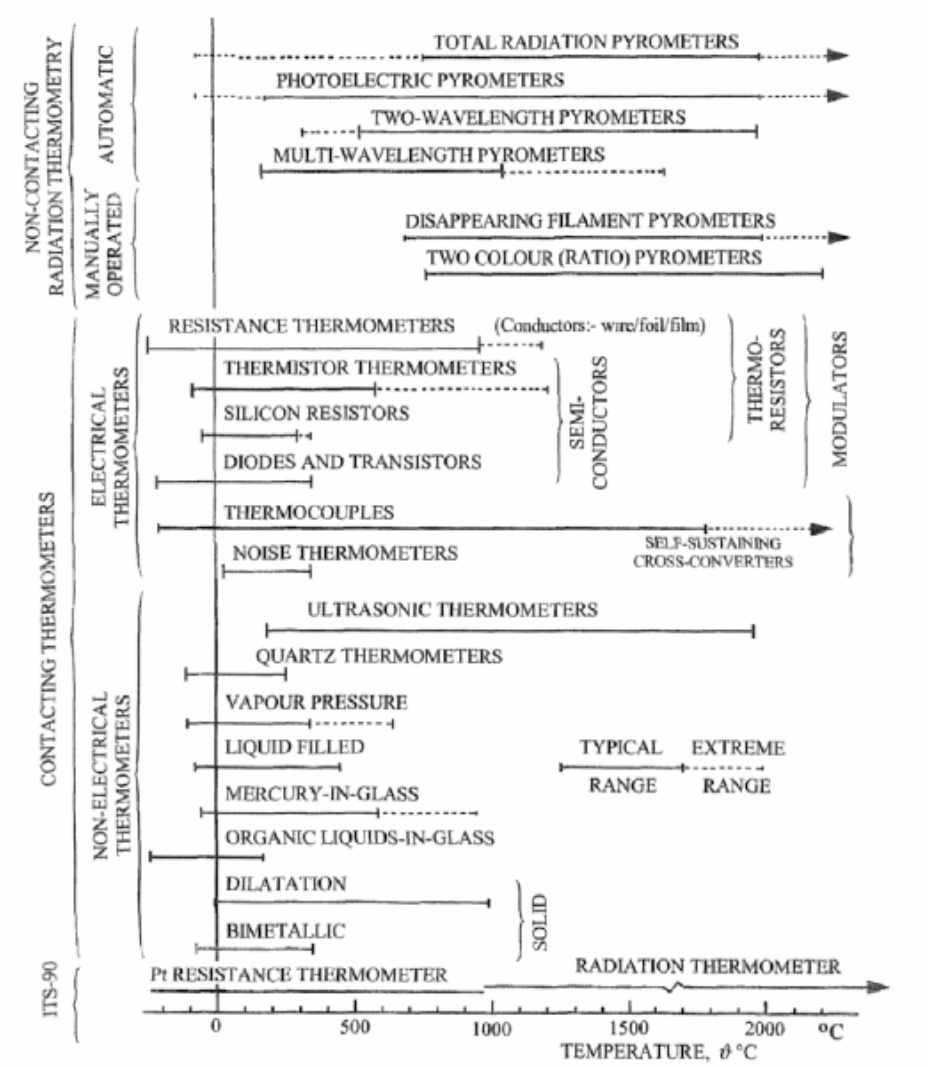

Figure 2.1 Classification of temperature measuring instruments/sensors by measuring range [5]

The international temperature scale of 1990 (ITS-90) is a standard adopted by international committee of weights and measures in 1989. The scale is established by correlating some temperature values with a number of well reproducible equilibrium states, which define the primary standards to be used. It can be observed from Figure 2.1 that thermocouples have the widest range of operating temperature. The various thermometers are classified and discussed in more detail below.

Two major classification of temperature sensors are contact temperature sensors and non-contact temperature sensors. Contact temperature sensors measure their own temperature. As the name suggests, they are in contact with the object and it is assumed or known that both are in thermal equilibrium, that is, there is no heat flow between them. Non-contact temperature sensors measure the thermal radiant power of the infrared or optical radiation that they receive from a known or calculated area on the object's surface, or a known or calculated volume within it.

Figure 2.2 – 2.4 shows the classification of temperature instruments [5]. The classification is based mainly on the physical quantity into which the temperature signal is transformed.

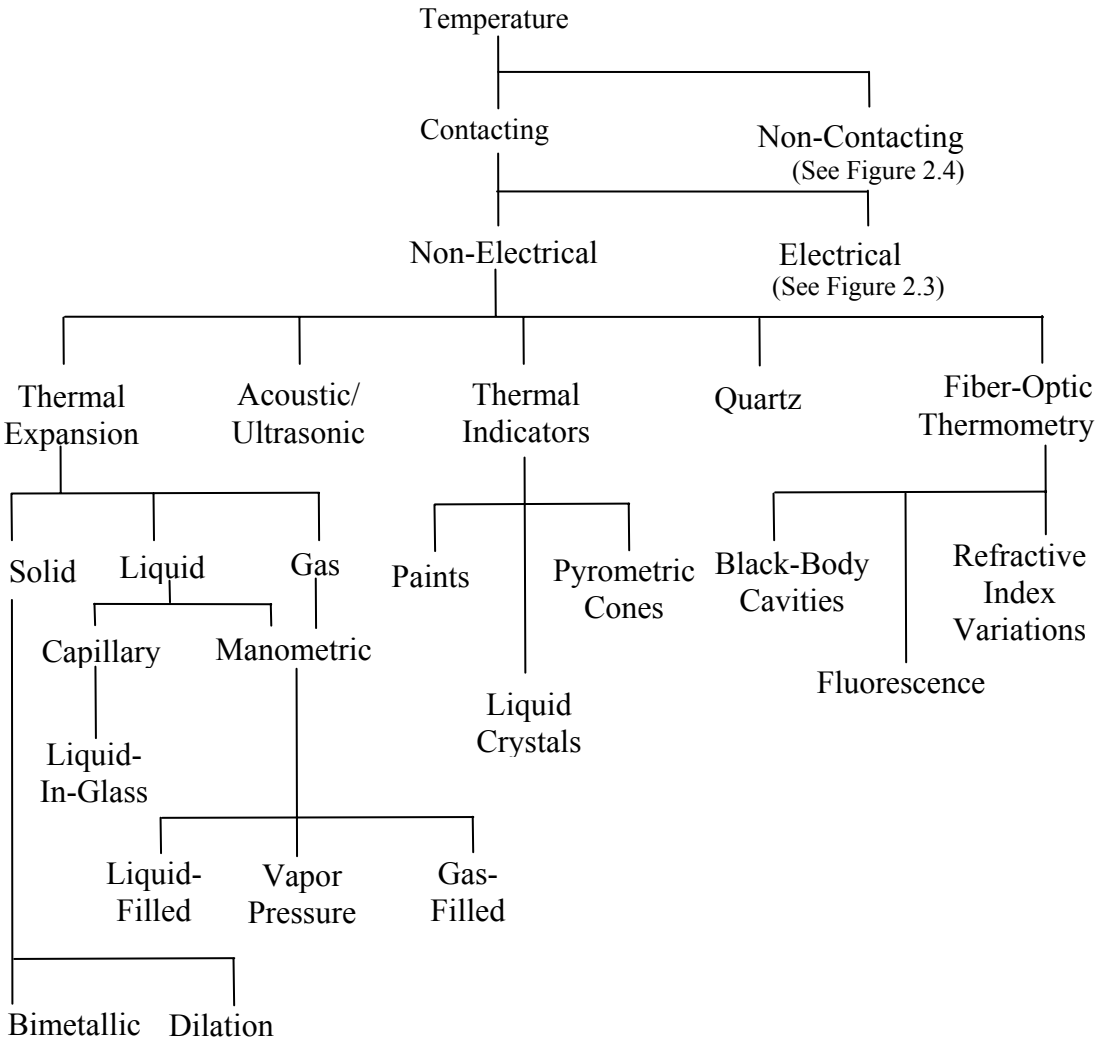

Figure 2.2 Classification of non-electrical contacting temperature sensors

Contact sensors function through conductive and convective heat transfer. Further grouping by the energy form of the output signal, distinguishes non-electrical sensors from the electrical group. Non-electrical sensors are classified in Figure 2.2 on the basis of thermal expansion of solids, liquids and gases. Electrical types of contacting thermometers are grouped in Figure 2.3.

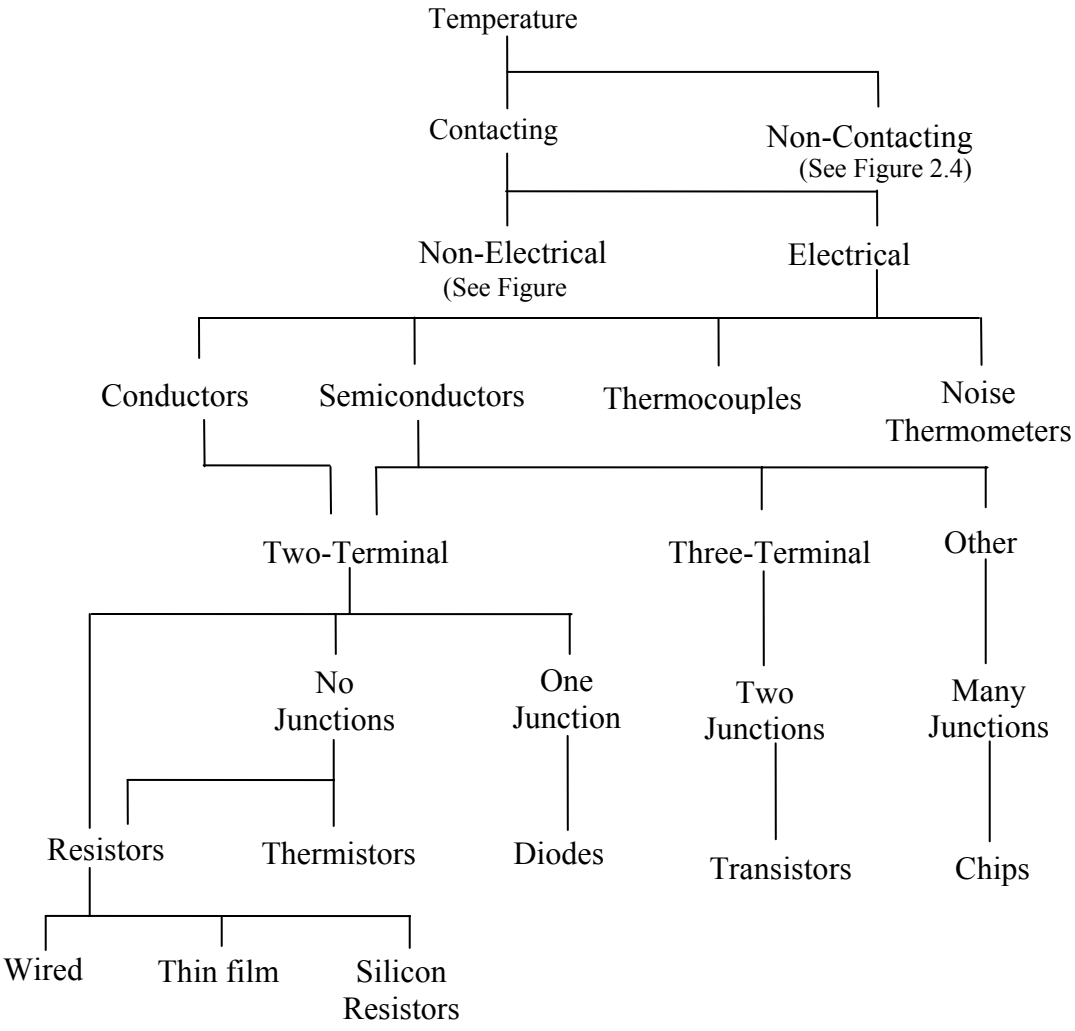

Figure 2.3 Classification of electrical group of contacting temperature sensors

A more detailed classification of non-contacting temperature sensors is shown in Figure 2.4. A distinction is made between those non-contacting methods, which use direct sensing, and those which apply interrogative methods. In the direct sensing group, the intensity of directly radiated energy is detected. For the interrogating group, an excitation signal is used to interrogate the body or object whose temperature is to be sensed.

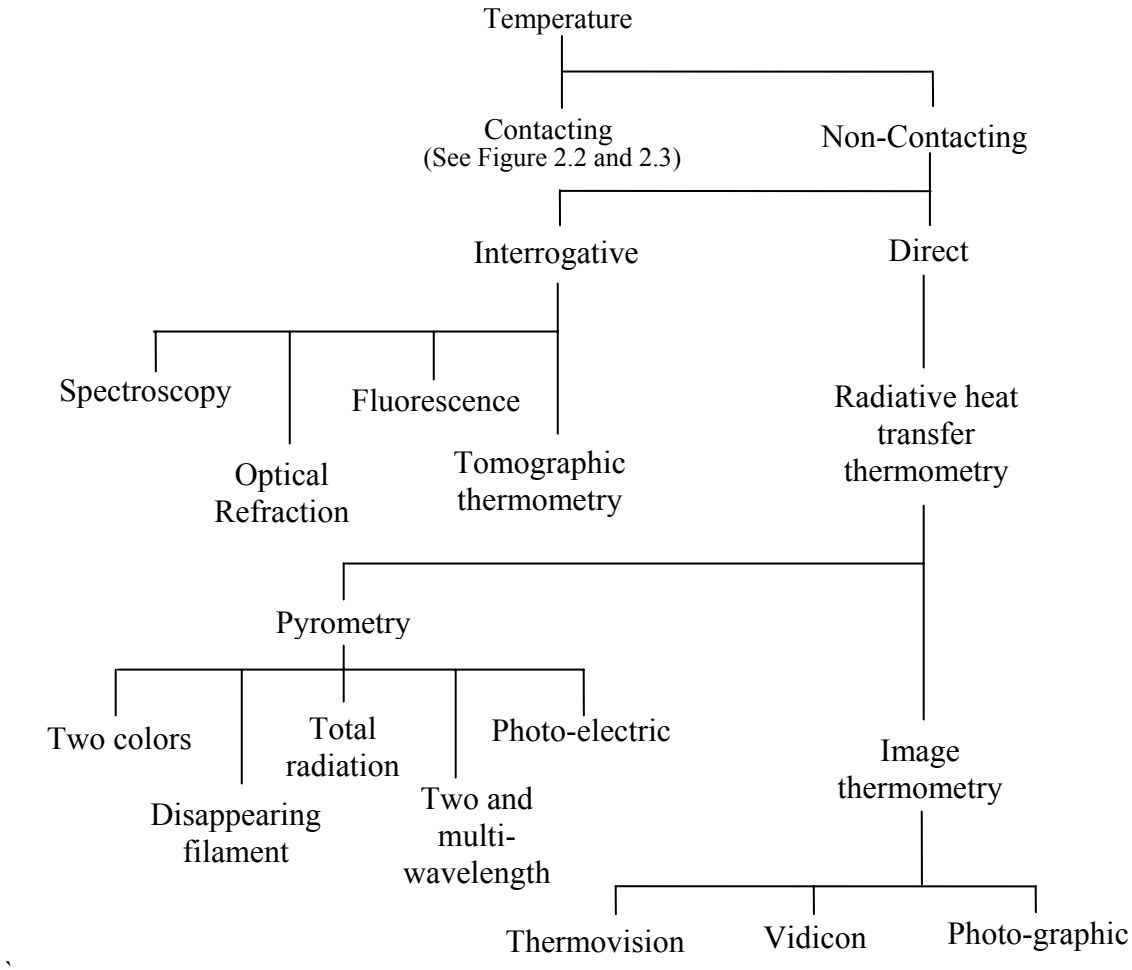

Figure 2.4 Classification of non-contacting group of temperature sensors

2.2.1 Non-electric thermometers

The classification of non electrical thermometers is shown in Figure 2.2. Liquid-in-glass thermometers are based on the principle of expansion and contraction of liquids with increasing and decreasing temperatures respectively. The selection of liquid is based on the temperature range for which the thermometer is to be used. They are most

frequently used within the temperature range -40˚C to +250˚C. These thermometers are accurate over a small range and the accuracy and resolution is determined by the length of the thermometer. Their disadvantages include slow response and fragility [5].

Thermometers using expansion of solids, like dilation and bimetallic thermometers use differences between the coefficients of linear thermal expansion of two different materials. Dilation thermometers, which can measure temperatures below about 1000˚C with errors of ±1% to ±2% of the temperature range, indicate the average value of temperature along their length. Useful temperature ranges that may be covered by bimetallic thermometers may be from -40˚C to +500˚C with errors between ±1% to ±2% of full scale. Bimetallic thermometers are simple and robust in structure and have low sensitivity to both vibration and electrical disturbances. Their dimensions vary from 250mm to 1m in length and 6mm to 10mm in diameter [5].

Temperature indicators allow estimation of temperature and cannot be used as precision measuring instruments. The most widely used indicators include pyrometric cones, thermochromic paints, temperature indicating crayons, self-adhesive indicators and liquid crystals. Self-adhesive indicators are miniature in size and are used to determine the temperature of small components such as transistors and integrated circuits. They have an application range from 30˚C to 280˚C.

Liquid crystals are compounds which change their reflection factor in the visible radiation range. They have been used for imaging thermal fields by applying a thin layer over the investigated surface in a 10μm to 20μm thick films. They have a resolution between 0.01˚C to 10˚C over a temperature range from -40˚C to +283˚C and response time of 0.5s – 2s [6]. The measurements are influenced by radiation reflected from the

investigated surface. Also these sensors require costly equipment to remotely measure temperature.

Fiber optic thermometers can be classified into two groups as intrinsic sensing thermometers and extrinsic sensing thermometers. In intrinsic sensing thermometers the optical fiber is itself used as the temperature sensor. In these sensors a light modulating property of the optical fiber is modulated by temperature. Extrinsic sensing thermometers use the optical fiber for transmission of electromagnetic waves between the sensor and the electronic temperature indicating system. Thermal radiation generated within a quartz fiber by hot spots can be used for sensing. Hot spots up to 1000˚C can be determined by 1mm thick quartz fiber [7]. Theses sensors are very costly and are strongly influenced by the physical environment.

Thermometers with Fabry-Perot sensors, which are one of the popular extrinsic sensing thermometers, operate on the principle of spectral dependence of the spectral reflection coefficient of a thin mono-crystalline Si film. These thermometers, which are immune to electromagnetic fields, operate in the temperature range from 0˚C to 400˚C [5]. The inherent disadvantage of this sensor is its instability. Also the film is easily degraded and requires very good packaging to ensure long life.

2.2.2 Electric thermometers

Electrical thermometers are broadly classified, as shown in Figure 2.3, as conductors, semiconductors and thermocouples. Thermocouples are one of the most-widely-used temperature sensors due to their wide operating range (1-2500K), stability, simplicity and lack of requirement of external power supply. Their accuracy is typically ±

0.1% – 1% of the full-scale reading [6]. One of the disadvantages of using thermocouples is two temperatures need to be measured. Also the materials of which thermocouple wires are made are not inert and the thermoelectric voltage developed along the length of the thermocouple wire may be influenced by corrosion.

Resistance thermometers use the temperature dependence of resistance of a material in temperature measurement. Resistance thermometer detectors (RTDs) consist of a conductor wound or deposited on an insulating support or former. Pure metals such as platinum, nickel and copper are used, since they guarantee reproducibility. Pt RTDs can be used in the temperature range -260˚C to +1060˚C [6]. RTD's are not as rugged and inexpensive as thermocouples. RTD's are also subjected to inaccuracies from self-heating.

Semiconductor thermometers are made from materials which are neither conductors nor insulators. Thermometers of this type, which may use bulk material temperature dependencies or junction effect carrier density relations, may be classified as bulk effect two-electrode sensors and junction device sensors. Bulk effect two-electrode sensors, which belong to the resistive group, possess no semiconductor junctions. They are thermistors or silicon RTDs. Junction device sensors are either diodes with one junction and two terminals, transistors with two junctions and three terminals, or integrated circuit sensors with multiple junctions and number of terminals.

Thermistors are non-linear, temperature dependent resistors with high TCR. In practice, only thermistors with a negative temperature coefficient (NTC) are used for temperature measurement. Thermistors are only suitable for use in the temperature range

from -80˚C to +200˚C [7]. They offer the advantages of being low in cost, highly sensitive and small in size.

Diodes and transistors are junction semiconductor devices for which current versus voltage characteristics are substantially determined by the relations between carriers on each side of a semiconductor region. For a given dopant concentration, the carrier density is strongly temperature dependent. The temperature measuring range of diode thermometers is limited by maximum permissible junction temperature and by the range of linearity of the output signal. Typical measuring range of Si diodes is -50˚C to +150˚C [5].

Integrated circuit temperature sensors are one of the latest innovations in temperature sensing. The main advantage to this type of sensor is that it can be designed to provide an output that is proportional to absolute temperature. The output of IC sensors is typically stated in microamps per degree centigrade. The disadvantages of IC sensors include fragility and a very limited temperature range, usually to 150°C maximum [8].

2.3 Micromachined temperature sensors

As technological improvements have been made, the world has become a smaller place. One primary objective of technological improvements is to make everything smaller and portable but with better performance and a lower power requirement. Miniaturized sensors have become an indispensable element in this endeavor.

The goal of this work is to develop a highly sensitive miniature temperature sensor that can withstand harsh environments. The applications of this research involve

silicon based devices hence a silicon based sensor is explored as it provides easy integration.

Micromachined temperature sensors have been actively researched in the recent past. Park et. al. have developed a micro temperature sensor array with thin film thermocouples to measure chip temperature distribution of electronic packaging [9]. The sensor array of 150nm thickness had 10x10 junctions within a 9x9 mm area and achieved a sensitivity of 17.6μV/˚C.

Miniature cryogenic resistance thermometers based on germanium films on gallium arsenide and silicon thermodiode temperature sensors have been investigated by Mitin et. al. [10]. The fabricated resistance thermometers covered the temperature range from 25mK to 300K, while the thermodiodes covered the 4 to 600 K temperature range. The resolution of the sensors has not been mentioned and the response is not linear.

Sazda et. al. have designed a compact silicon temperature sensor for determination of blood perfusion in bio materials [11]. The circuit is based on proportional-to-absolute-temperature principles. A feedback technique is used to improve linearity and reduce noise. A resolution of 0.003˚C was achieved by this sensor in the 30˚C to 50˚C temperature range.

2.3.1 Bulk silicon based temperature sensors

A bulk silicon based temperature sensor has been designed and fabricated by Gupta et. al. [12]. The sensor had a linear response over a temperature range -50˚C to 150˚C. TCR and sensitivity of the sensor were found to be 3.76 x 10-3 $^{\circ}C^{-1}$ and 1.24Ω/˚C, respectively.

Qiu et. al. have fabricated a low-cost broad range silicon temperature sensor [13]. Copper was doped in silicon to alter its properties. The sensors working range covered 25˚C to 500˚C with an exponential like functional dependence. A charactersistic of this sensor is that it had three linear regions in its response and each region could be used for a different range of temperature. The resolution of this sensor is not stated but the response shows that the maximum change in conductivity is from 0.1mho.cm^{-1} to 1.7mho.cm^{-1} over the temperature range 320˚C to 530˚C.

Kewell et. al. have described a temperature sensor which operates over the range 40 -150 K [14]. The measurement principle is based on the analysis of the time decay of the luminescence emitted by erbium-doped silicon. This sensor requires bulky and costly equipment for its measurement purposes and is not a very good commercial solution.

2.4 Current work

As mentioned earlier, the motivation for this research is to develop a temperature sensor which is sensitive, robust and can be fabricated using micromachining techniques. The most measured temperatures of ocean lie in the 0˚C to 30˚C range. For the magnetocaloric microcooler currently under development the temperature ranges of interest are -20˚C to 20˚C.

These applications require a sensor that is highly sensitive and can withstand harsh environments (CTD sensor). The sensors that have been discussed above are not the best fit as they do not possess the sensitivity in the required temperature range and are not cheap.

This work focuses on the development of a bulk silicon based temperature sensor that can be easily packaged for harsh environments, operate at low temperatures and possess high sensitivity and resolution. High sensitivity is obtained by diffusing gold in silicon to alter its electrical properties. The influence of the diffusing environment on the sensor is studied to develop sensors for specific ranges and applications.

CHAPTER 3

THEORY

Properties of semiconductors are significantly affected by presence of impurities. The change in properties is due to the impact of impurities on the band structure of semiconductors. Impurities are added to semiconductors in controlled amounts for fabrication of solid state devices.

3.1 Semiconductor operation to provide enhanced sensitivity

Enhanced sensitivity can be obtained from semiconductors if they are not operated in the saturation region. Figure 3.1 shows the carrier concentration of a semiconductor plotted in a log scale against reciprocal temperature for a 50 Ω-cm n-type silicon wafer. A majority of semiconductor devices operate in the saturation region of this curve, where the temperature coefficient of resistivity is governed by the carrier mobility and the effective density of states function. To get increased sensitivity the device needs to be operated in the intrinsic and freeze-out region, as the carriers show marked sensitivity to temperature in these two regions [15]. The higher sensitivity in the intrinsic region cannot be utilized due to high temperatures.

Adding deep impurities will shift the freeze-out region horizontally to the left. Deep impurities drive the sensor operating temperatures for high sensitivity out of the

cryogenic temperatures to relatively high temperatures. Proper control of the impurities can be used to change the slope of the freeze-out region to match the highly desirable slope of the intrinsic region. Impurities can be added to silicon either during crystal growth or by diffusion.

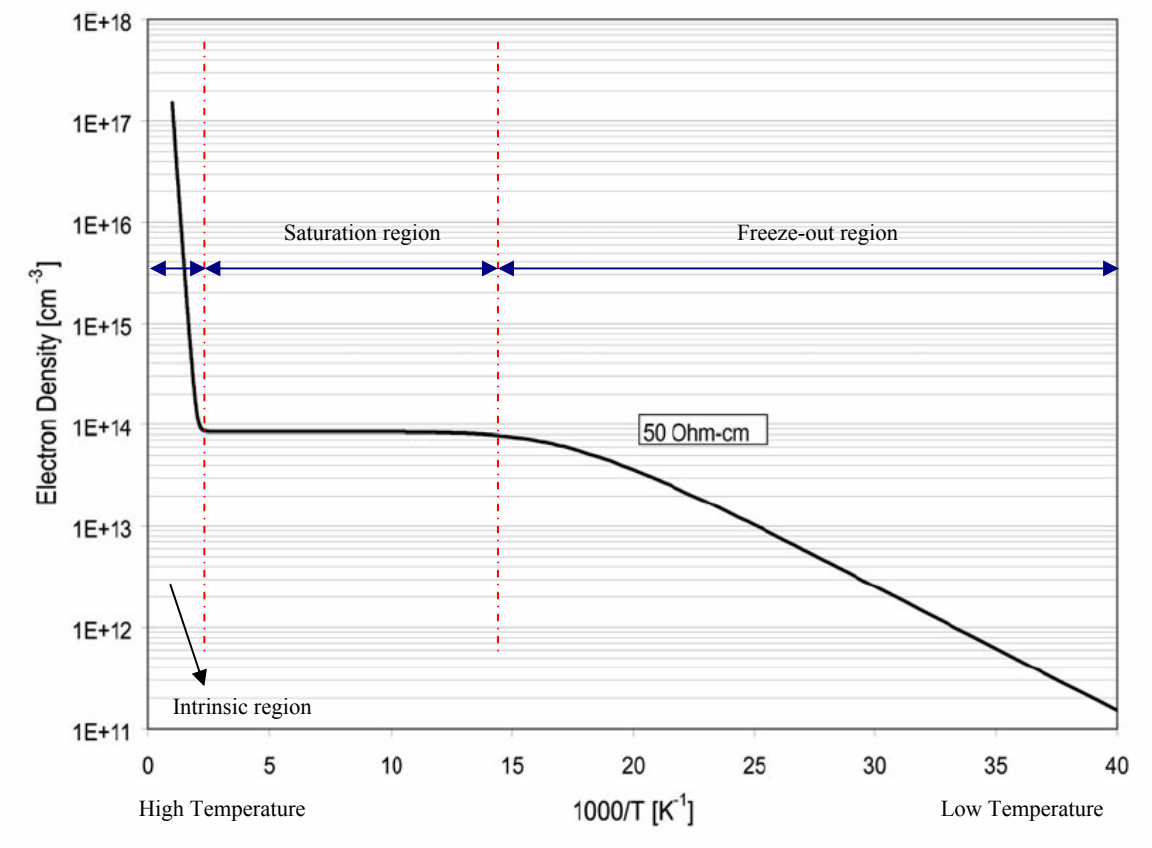

Figure 3.1 Carrier concentration against the reciprocal temperature for Si with resistivity 50Ω-cm [15]

3.2 Diffusion

Diffusion is a process where material is transported by atomic motion. In conduction of heat, heat transfer is a result of a temperature gradient. Diffusion is transportation of molecules from a high concentration to a low concentration. Mass transport in gas and liquid involves flow of a fluid although atoms also diffuse. Solids on

the other hand support shear stresses and hence do not flow except by diffusion involving jumping of atoms to a fixed network of sites.

3.2.1 Diffusion process

Diffusion processes may be divided into two types: (a) steady state and (b) nonsteady state. Steady state diffusion takes place at a constant rate, i.e. independent of time. Nonsteady state diffusion is a time dependent process in which the rate of diffusion is a function of time. Both types of diffusion are described quantitatively by Fick's laws of diffusion [16]. Fick's first law may be formulated as

$$J = -D\left(\frac{dc}{dx}\right) \tag{3.1}$$

Fick's first law in words is: *The diffusive flux is proportional to the existing concentration gradient*. In the above equation J represents the flux (of matter), D is diffusivity or diffusion constant and $\left(\frac{dc}{dx}\right)$ is the concentration gradient. The diffusion constant (D) reflects the mobility of the diffusing species in the given environment.

Fick's second law concerns nonsteady state diffusion and is formulated as

$$\frac{dc}{dt} = D\frac{d^2c}{dx^2} \tag{3.2}$$

This relationship states that *the rate of compositional change is proportional to the rate of change of the concentration gradient*.

3.2.2 Diffusion in solids

Diffusion in solids can be broadly classified in two categories, namely self-diffusion and interdiffusion. Self-diffusion is migration of *host* atoms through their own lattice and interdiffusion is migration of *impurity* atoms in the *host* lattice.

3.2.3 Mechanism of diffusion

The two main diffusion mechanisms are vacancy diffusion and interstitial diffusion (Figure 3.2). Vacancy diffusion (or substitutional diffusion) involves migration from a normal lattice position to an adjacent vacancy. Self-diffusion occurs by this mechanism. Interstitial diffusion involves migration of interstitial atoms to neighboring empty interstitial sites. This mechanism is common for interdiffusion of impurities. Interdiffusion can also occur due to vacancies.

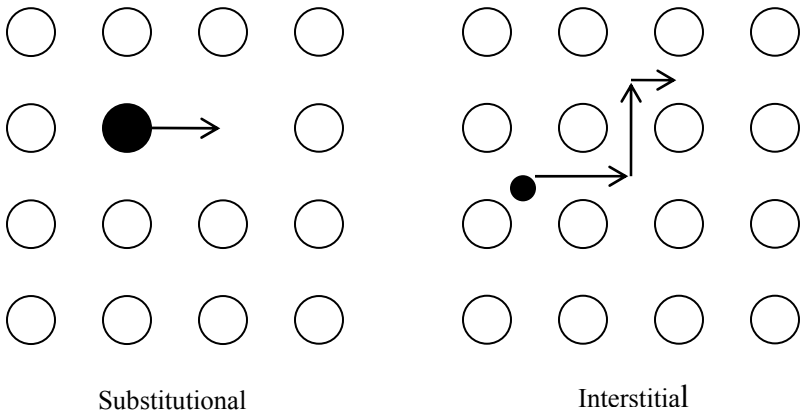

Figure 3.2 Mechanism of diffusion

3.2.4 Factors influencing diffusion

Diffusion is dependent on various parameters. The important factors that influence diffusion are temperature, diffusion mechanism, the diffusing and host species and microstructure.

Diffusion constant (D) is the measure of mobility of diffusing species and can be calculated by

$$D = D_o \exp\left(-\frac{Q_d}{kT}\right) \tag{3.3}$$

where D_o is temperature-independent pre-exponential, Q_d is the activation energy for diffusion, k is the boltzmann's constant and T absolute temperature [17]. Diffusion rates increase with increasing temperature. The activation energy Q_d and pre-exponential D_o can be estimated by plotting log D versus 1/T and using the following equations.

$$\log D = \log D_0 - \frac{Q_d}{2.3k}\left(\frac{1}{T}\right) \tag{3.4}$$

$$Q_d = -2.3k\left[\frac{\log D_1 - \log D_2}{1/T_1 - 1/T_2}\right] \tag{3.5}$$

Interstitial diffusion is usually faster than vacancy diffusion because bonding of interstitials to the surrounding atoms is generally weaker and also there are many more interstitial sites than vacancy sites to jump to.

The diffusing and host species also play an important role in the diffusion. Smaller atoms diffuse more readily than big ones, and diffusion is faster in loosely packed crystals as compared to the tightly packed.

More open atomic structure at defects (grain boundary, dislocations) can lead to higher mobility of atoms along the defects. The activation energy for grain boundary diffusion is significantly lower than the bulk.

3.3 Diffusion in silicon

Elements diffusing in silicon are frequently classified as “slow” or “fast” diffusers. Slow diffusers have diffusion coefficients reasonably close to those of self diffusion, whereas fast diffusers have diffusion coefficients that are many orders of magnitude larger than those of slow diffusers at a given temperature.

The large difference in the diffusion rates of the slow and fast diffusers is mainly due to the different diffusion mechanisms. Slow diffusers, such as the common group III and group V dopants, are substitutionally dissolved and require intrinsic point defects (vacancies and/or self interstitials) for their diffusion. Fast diffusers like Cu, Li, H, Fe, Au and O are predominantly interstitially dissolved and move by jumping from one interstitial site to other without requiring intrinsic point defects. Figure 3.3 shows the impurity diffusion coefficients in silicon for fast diffusers [18].

3.4 Effect of diffusion of deep impurities

When an impurity (dopant) is added/diffused in silicon it reduces its resistivity. Depending on the dopant diffused, n-type or p-type silicon is obtained. In n-type silicon, electrons are the majority carriers whereas in the case of p-type silicon it is holes. Phosphorus (P) and arsenic (As) are the major dopants used to obtain n-type silicon. These introduce a shallow donor level in silicon bandgap. The resistivity of silicon can be increased by compensation of the introduced donors.

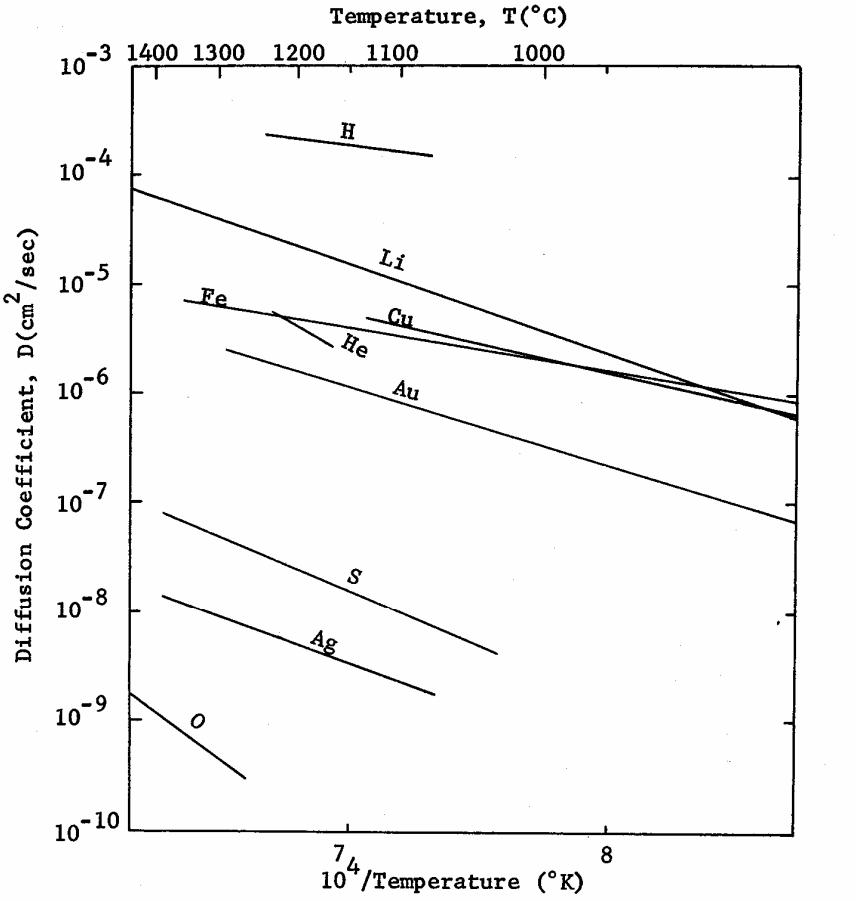

Figure 3.3 Impurity diffusion coefficients of fast diffusers in silicon [18]

A deep acceptor (DA) level when introduced will increase the resistivity of silicon. The resistivity will increase as the density of DA's is increased. When the concentration of DA's is low, resistivity is low due to insufficient number of deep acceptors, which causes undercompensation. Resistivity is highest when the ionized DA's exactly compensate the shallow donor background. When the density of DA's is higher than the donors, the resistivity reduces due to large number of ionized acceptors leading to overcompensation of n-type background and the material tends to become p-type.

In principle, although a shallow p-type dopant such as boron (B) is capable of compensating the P (n-type) background, the control required over the density of B

doping is too tight to be achievable in practice. In the case of DA the acceptor level is near the Fermi level, and only a small fraction of the DA density is ionized. As a result, the compensation changes gradually with change in number of DA's (N_{DA}). The inference from the above discussion is that a relatively shallow DA can compensate a shallow donor background only when N_{DA} is nearly equal to number of donors (N_D), but for a sufficiently deep DA, resistivity remains high over a large range of N_{DA} for $N_{DA}>N_D$.

Introduction of DA's has some limitations in the sense that it is extremely difficult to introduce an exact concentration of an impurity. A possible solution is to make up for the overcompensation due to an excess DA by co-doping with a deep donor (DD). The resistivity will be highest when the density of ionized DD is approximately equal to that of overcompensating DA, and no longer depends on the uncontrolled shallow donor background [19].

Figure 3.4 shows the energy levels of impurities in silicon. In Figure 3.4 E_c represents the conduction band and E_v represents the valence band of silicon. The bandgap of Si is 1.12 eV at room temperature. Almost all transition elements introduce a pair of DD and DA in the Si bandgap. A possible means of controlled co-doping of Si with a DD and a DA is to use a transition metal impurity like gold.

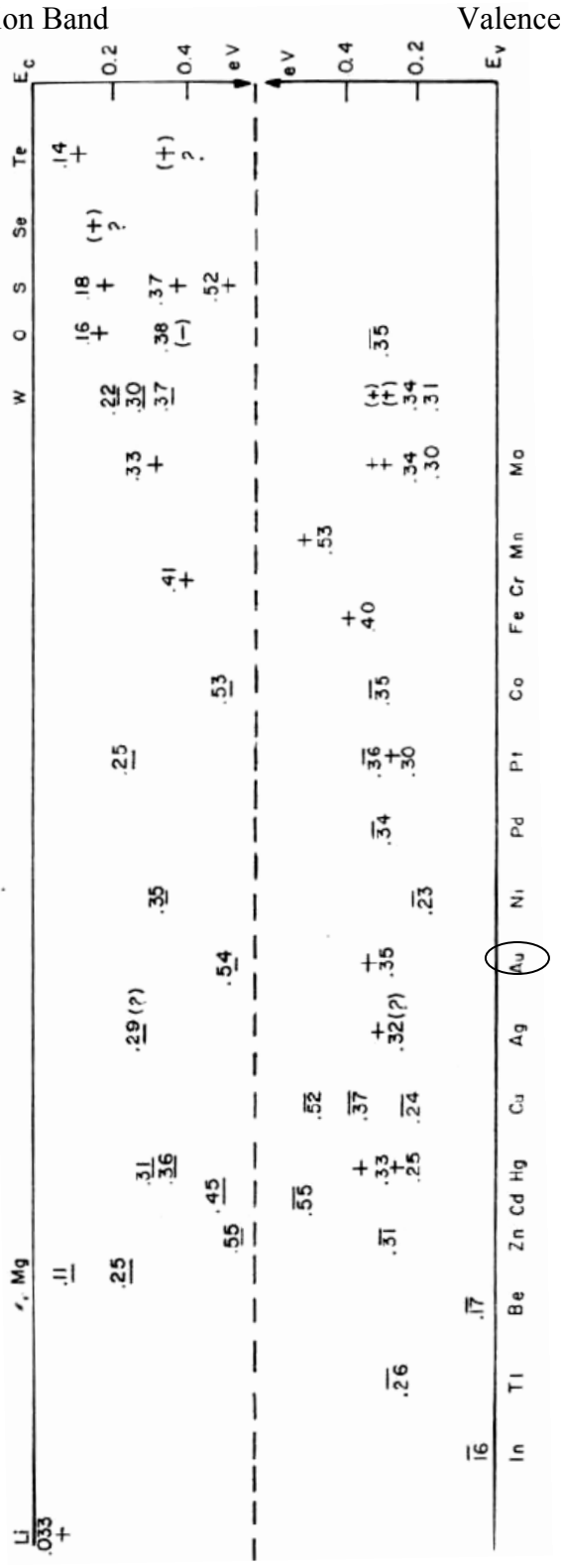

Figure 3.4 Deep energy levels in silicon [20]

3.4.1 Gold diffusion in silicon

Gold is a stable transition metal having density 19.3 gm/cm^3, but is a very fast diffuser in silicon. Gold diffuses in silicon by substitutional-interstitial diffusion above 800˚C, where it is predominantly substitutionally dissolved but diffuses interstitially [21]. The basic mechanisms of substitutional-interstitial diffusion are Frank-Turnbull mechanism and kick-out mechanism. In the case of Frank-Turnbull mechanism, changeover of A-atoms, where A is the diffusing species, from interstitial sites (A_i) to substitutional sites (A_s) requires vacancies (V).

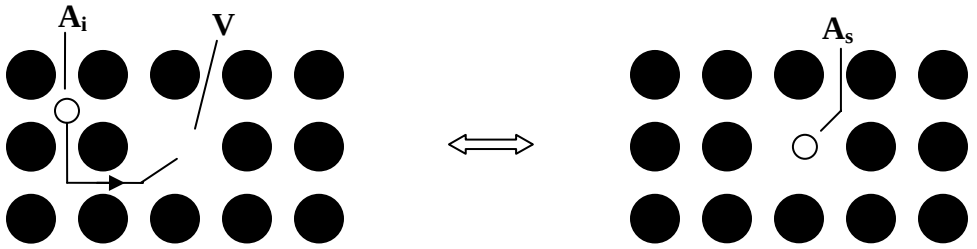

a) Frank – Turnbull mechanism

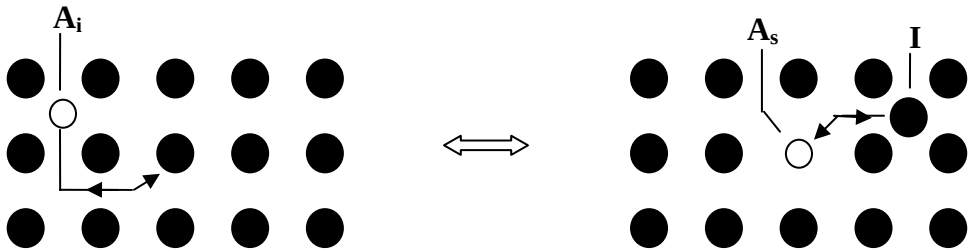

b) Kick - out mechanism

Figure 3.5 Frank-Turnbull and kick–out mechanism

If all species are uncharged then the changeover reaction involving vacancies is described by

$$A_i + V \Leftrightarrow A_s \tag{3.6}$$

The analogous reaction involving self-interstitials (I)

$$A_i \Leftrightarrow A_s + I \tag{3.7}$$

is termed as the kick-out mechanism. Both mechanisms are schematically indicated for an elemental semiconductor in Figure 3.5.

Au diffusion in silicon at and above 800˚C is dominated by kick-out mechanism. Since Au diffuses by an interstitial-substitutional mechanism, Au diffusion is strongly influenced both by crystal perfection and by the presence of other impurities. The dislocations may act as sinks or self-interstitials and therefore enhance the local incorporation rate of Au_s.

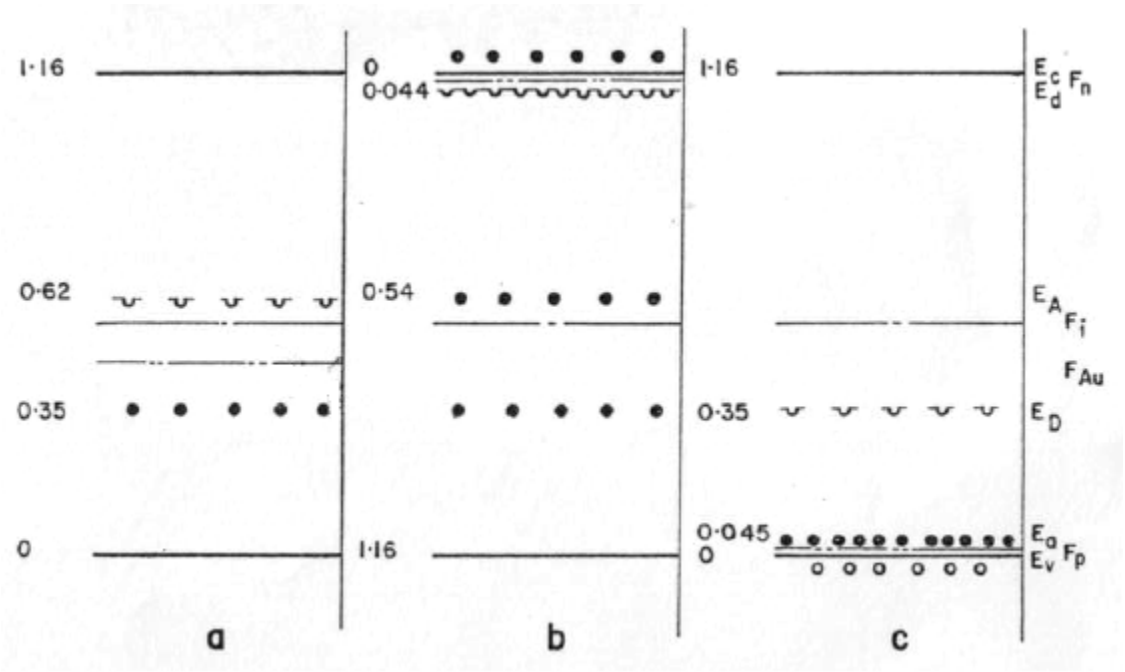

Figure 3.6 Energy band diagram (in eV) for silicon doped with gold: (a) no other impurity present, (b) shallow donor present, (c) shallow acceptor present [22]

Au introduces an acceptor level 0.54eV below the conduction band edge and a donor level 0.35eV above the valence band edge in Si to pin the Fermi level at the middle

of the Si bandgap. A schematic diagram of these levels is shown in Figure 3.6 for different doping conditions. In the Figure 3.6 E_a and E_d represent the energy level of the shallow acceptors and donors respectively and E_A and E_D represent the energy levels of gold.

Near absolute zero, essentially all the lower gold levels (donors) are filled and upper gold levels (acceptors) are empty. At higher temperatures such as room temperature the electrons will be distributed according to their degeneracy. In silicon doped with N_d per cm^3 shallow donor (e.g. phosphorus), the Fermi levels in the extrinsic temperature range is close to the conduction band. At room temperature nearly all the shallow donors will be ionized so that the free electron concentration n is equal to the donor concentration N_d.

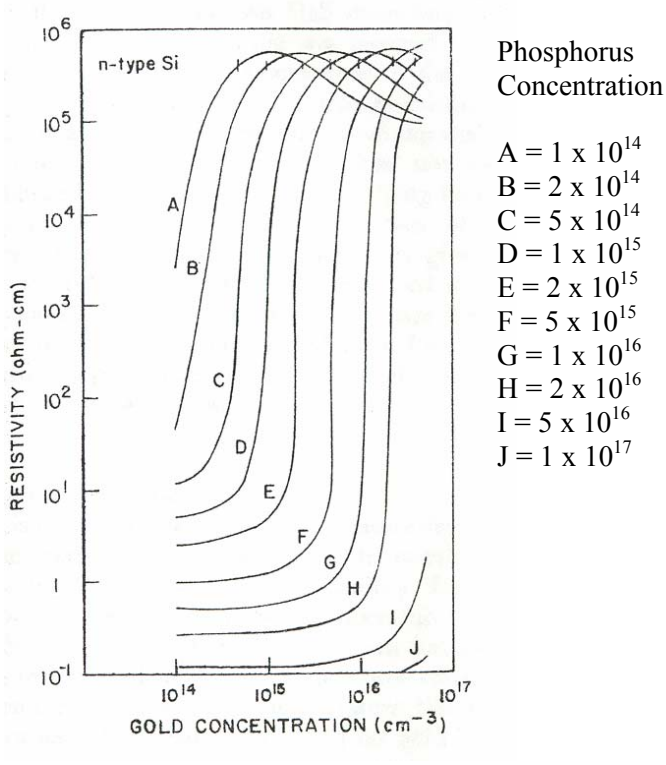

Figure 3.7 Resistivity vs. gold concentration at 300K in n-type silicon [22]

As the gold is added, these electrons will fill the upper gold levels. When the gold concentration equals the shallow donor concentration the free electron density will drop sharply, the Fermi level will approach the intrinsic value and the resistivity will increase rapidly as shown in Figure 3.7 [22]. Also as the concentration of initial dopant (phosphorus) increases the curve shifts horizontally towards the right.

As still more gold is added, the electron concentration will continue to decrease, the Fermi level will pass below its intrinsic value, and the resistivity will reach its maximum when the electrons and holes contribute equal to the conductivity, $n\mu_e=p\mu_h$, where n (p) is the number of electrons (holes) and μ_e (μ_h) is the mobility of electrons (holes). Further addition of gold will cause the material to be distinctly p-type and the resistivity to decrease toward the value obtained when gold is the dominant impurity.

3.5 Temperature sensing using doped silicon

The resistivity of a material which is a function of lattice temperature, is given by

$$\rho = \frac{1}{q\left(\mu_e(T)n_e(T) + \mu_p(T)n_p(T)\right)} \tag{3.8}$$

where q is the charge of the electron (C), n_e (n_p) the free electron (hole) density (cm^{-3}) in silicon, μ_e (μ_p) the mobility of electron (hole) (cm^2/V-s) in silicon and ρ the resistivity (Ω-cm) of silicon [15]. Both carrier concentration and carrier mobility are temperature dependent. The free carrier concentration at room temperature is equal to the doping concentration, but at higher temperatures the thermally generated carriers dominate, raising the carrier concentration substantially above the doping level.

For lightly doped samples, the lattice scattering dominates, and the mobility decreases with increasing temperature. For heavily doped samples, the effect of impurity

scattering is most pronounced at low temperatures. Therefore mobility increases as temperature increases. For a given temperature, the mobility decreases with increasing impurity concentration, because of enhanced impurity scattering. A 20 Ω-cm n-type sample when diffused with gold exhibits high resistivity which varies with temperature [23]. A temperature increase leads to reduction in resistivity, as shown in Figure 3.8, of silicon. It can be observed from Figure 3.8 that the resistivity changes from 10^5Ω-cm to 10^3Ω-cm over a temperature range of 300K to 400K. This indicates a highly sensitive resistivity change to temperature which forms the basis of the current work.

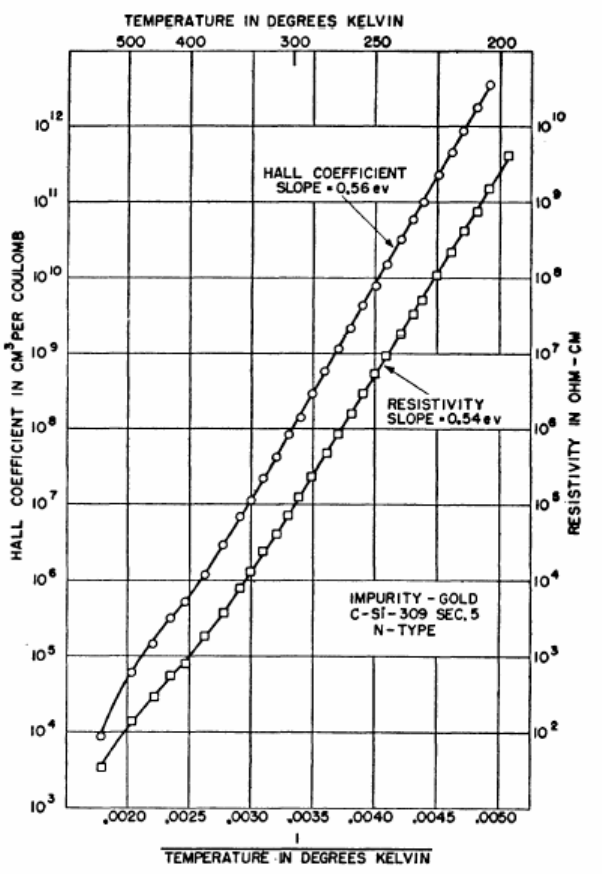

Figure 3.8 Effect of temperature on gold diffused n-type silicon [23]

CHAPTER 4

FABRICATION

In this chapter the fabrication of the temperature sensor is presented. Also discussed here are approaches to design, sensor issues and measurement setups.

4.1 Sensor development

One of the main goals of this research was to develop a high resolution temperature sensor that can be easily integrated with other devices and also be used in harsh environments. Packaging is the key for a sensor to be functional in any application. In the case of harsh environments, packaging becomes a critical aspect.

In this research, diffusion based low-cost bulk temperature sensor was attempted as it lends to easy fabrication and can be easily integrated with other Si based micromachined devices.

Two approaches were adopted for the sensor development. In the first approach the resistivity of the sensor was calibrated and related to the temperature change. Though the results were encouraging, it would be difficult for these measurements to be done in the applications intended. In the second approach the diffused wafer was treated as a resistor and the resistance change with temperature was measured and calibrated to relate to temperature.

4.2 Fabrication

In this work 250 μm thick, n-type (100) Si wafer with initial resistivity 10-20 Ω-cm was used for the fabrication of the temperature sensor. This base resistivity was chosen to be close to the CMOS standards because that would make the integration of this sensor to devices and systems easier. Gold was diffused to alter the electrical properties of silicon which was then used as the temperature sensor.

The initial approach for the fabrication of the sensor was to diffuse gold on a Si wafer and measure the change in the resistivity with temperature. Gold was deposited on Si wafer using e-beam evaporation. It has been suggested that near 1000˚C one monolayer of pure gold at the surface is large enough to saturate a 500 μm thick silicon sample [24]. Hence in this work, 250Å of gold was deposited for fabrication of the sensors with the rationale that there would be adequate gold for diffusion. The deposition was followed by diffusion in an open tube furnace for 2 hours in an oxygen environment. Gold diffusion from single side of the silicon wafer results in a U-shaped profile, consisting of an essentially symmetric profile with a flat minimum in the center of the sample, and increasing Au concentration at both surfaces [24]. The time and temperatures of diffusion was varied to investigate their effects.

The resistivity of the sample before and after diffusion was measured using a four point probe. Temperature dependence of resistivity was also measured and this was calibrated to measure temperature.

It would be difficult to continuously measure the resistivity of the wafer in certain environments like water (for oceanic applications). Another drawback of diffusing gold

throughout the wafer is the properties of silicon are altered and micromachining of the diffused wafer is not same as n-type or p-type silicon that is normally used.

To make a sensor that can be fabricated on the same silicon chip with other micromachined structures a different fabrication approach was chosen. In the second approach, gold was diffused only in certain regions of the wafer using shadow masks. This ensured lesser change in properties of silicon around the diffused regions. The dimensions of the shadow masks are shown in Table 4.1 and Figure 4.1 shows them.

Table 4.1 Shadow mask dimensions

Shadow Mask	Window Dimensions (in mm)
M1	10 x 5
M2	10 x 2
M3	5 x 2

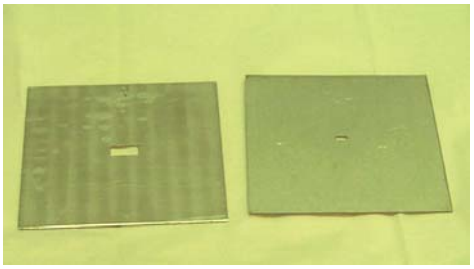

Figure 4.1 Shadow masks

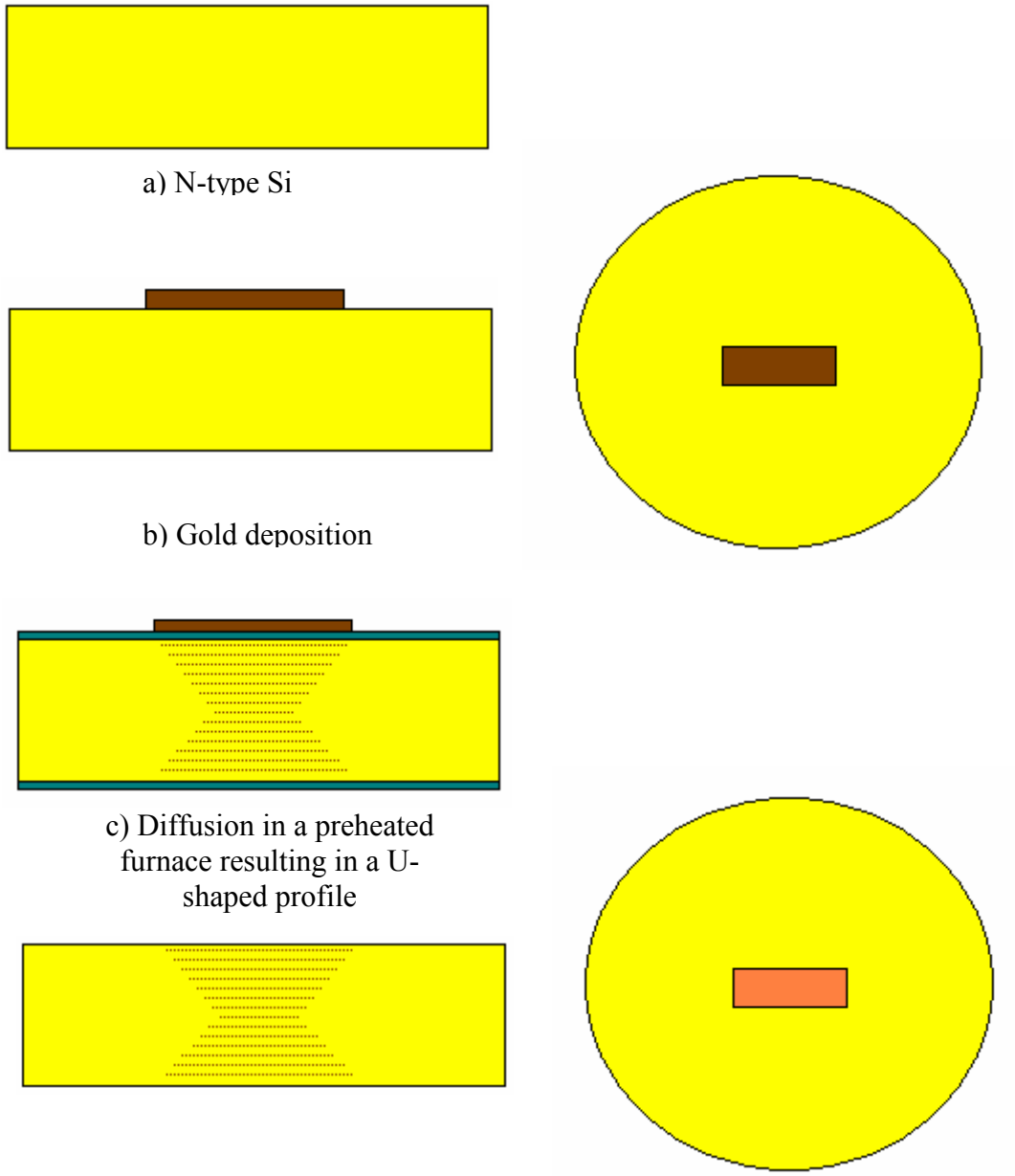

Figure 4.2 Process flow for diffusion of gold in silicon

Figure 4.2 shows the process flow for the fabrication of the temperature sensor. 250Å of gold was deposited on certain regions of the wafer using shadow masks, in an e-beam evaporator. The deposition pressure in the e-beam evaporator was 10^{-5} Torr. To

understand the parameters better a 2-inch silicon wafer was cut into 4 pieces and on each piece a different area (shadow mask M1, M2 and M3) area was deposited with gold. The deposited wafers were then diffused simultaneously.

Diffusion was done in a pre-heated furnace in both oxygen and nitrogen environments. The temperature of diffusion was also varied. The time of diffusion was kept constant as 2 hours for all fabrications. The wafers after diffusion were allowed to cool to room temperature outside the furnace. It was observed that an oxide layer formed in both the oxygen and nitrogen ambient. As an open tube furnace is used for diffusion oxygen from atmosphere results in formation of a thin oxide layer in the case of nitrogen ambient. Also there was excess gold present on the diffused area. The residual surface gold was then etched in gold etchant solution. Removal of surface oxide was done by a buffered oxide etch (BOE) step.

Diffusion was done in varied ambient and at different temperatures to study their respective effects. Table 4.2 shows the parameters that were used for the sensor fabrication. The values of M1, M2 and M3 can be referred to Table 4.1.

Table 4.2 Fabrication parameters

Sample	Ambient	Temperature (˚C)	Mask
S1	O_2	1000	M2
S2	O_2	1050	M1
S3	O_2	1050	M2
S4	O_2	1050	M3
S5	O_2	1100	M2

Table 4.2 Continued

S6	N_2	1000	M2
S7	N_2	1050	M1
S8	N_2	1050	M2
S9	N_2	1050	M3
S10	N_2	1100	M2

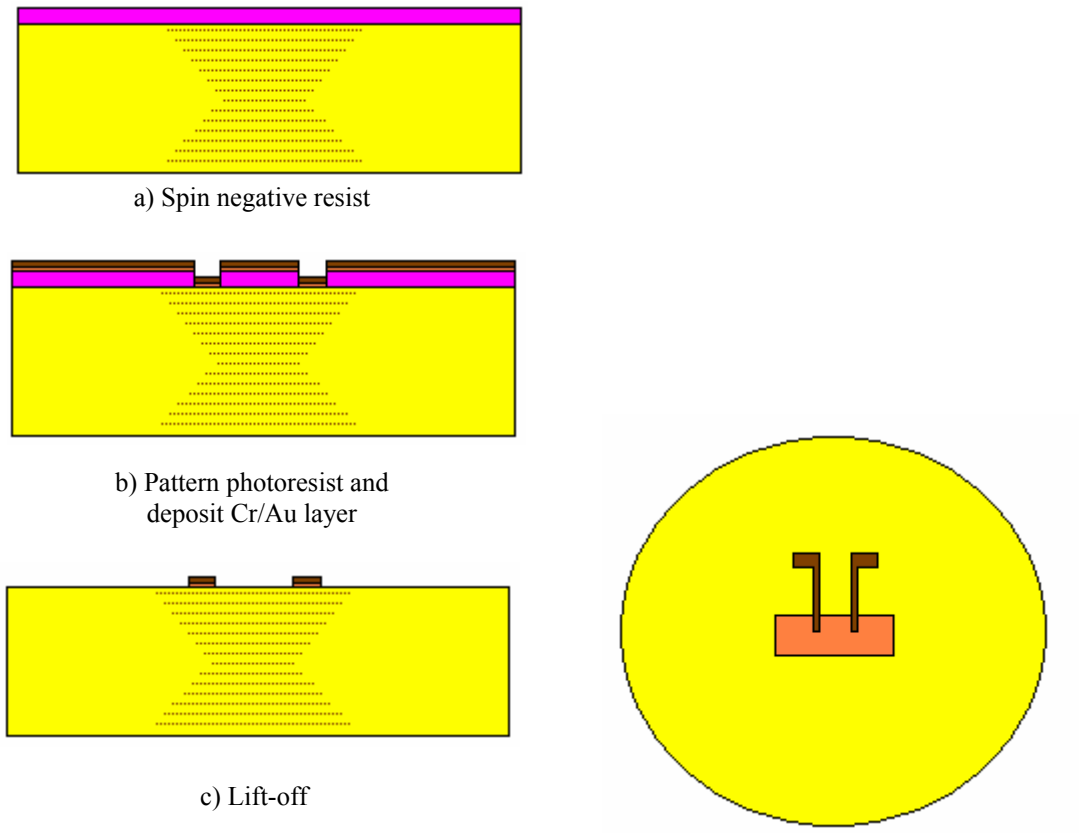

Figure 4.3 Process flow to pattern ohmic contacts

Ohmic contacts were patterned on the sensor using lithographic techniques as shown in Figure 4.3. Negative photoresist was spun on the diffused wafer and patterned

using a light field mask. 100Å of Cr was deposited followed by a deposition of 1500Å of Au by thermal evaporation on the patterned wafer followed by lift-off to form the ohmic contacts. The fabricated wafer with the ohmic contacts is shown in Figure 4.4.

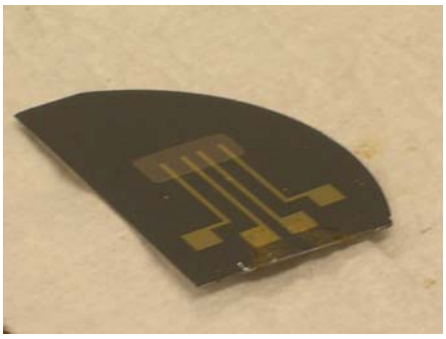

Figure 4.4 Fabricated temperature sensor

4.3 Measurement setup

The initial measurements were to calibrate resistivity of the temperature sensors. A four point probe was used for the measurements. Figure 4.5 shows the measurement setup. Source current in the range of 4.53×10^{-4} A to 4.53×10^{-6} A was applied and the resultant output voltage was measured. The diffused wafer was placed on a hot plate to measure the effect of temperature on resistivity. The temperature of the hot plate was logged with a thermocouple. The plate temperature was ramped up and it was assumed that the temperature of silicon was same as the hot plate.

Sheet resistance was calculated with the assumption that the gold diffused throughout the wafer and the bulk resistivity was calculated by the formula

$$\rho = 4.53t\frac{V}{I} \tag{4.1}$$

where ρ is the resistivity (Ω-cm), t is the thickness of the wafer (cm), I the source current (A) and V the measured voltage (V) [25].

For the second approach the fabricated sensor was designed to act as a resistor and the resistance was measured. The sensor was placed in a liquid and the temperature of liquid was varied to measure the effect of temperature on resistance. To ensure accurate readings it was necessary for the fluid to be highly resistive and not contribute to the measurements. DI water was chosen as the testing fluid due to its favorable properties.

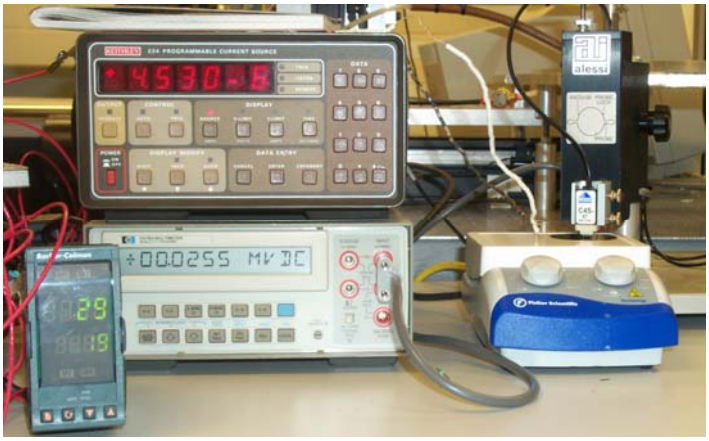

Figure 4.5 Measurement setup to measure effect of temperature on resistivity

The sensor was connected to a Keithley 2400 sourcemeter and placed in a beaker with DI water. The temperature of the DI water was varied by placing the beaker on a hot plate. To ensure uniform heating the liquid was constantly stirred at 300 rpm. The temperature of the hot plate was ramped up and measurements were taken as the liquid temperature increased.

The drawback of the aforementioned measurement techniques was the inability to do low temperature measurements (below room temperature). As the sensor needs to measure the temperature changes close to 0˚C, it was imperative to calibrate the sensor in that range. Also the measurements were not very stable as the values were dependent on

the surrounding parameters like humidity as the reservoir in which the testing was done was open to atmosphere. Hence another approach for measurements was implemented.

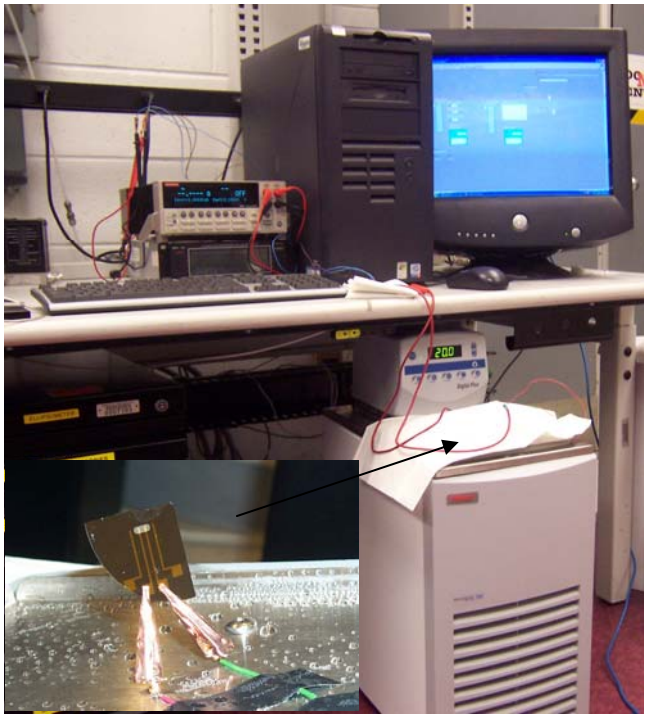

Figure 4.6 Measurement setup to measure temperature and resistance using labview

In this approach a Thermoelectron's neslab RTE-740 refrigerated bath was used to attain low temperatures. The sensor was placed in the reservoir of the bath, by attaching it to the lid of the reservoir as shown in Figure 4.6. DI water was used as the reservoir fluid. The resistance measurements were done with a Keithley sourcemeter. The current for the measurements was fixed to 1μA. The temperature of the bath was ramped up/down manually and the measurements were taken while the bath temperature ramped up/down. Labview version 7.0 was used to log simultaneously resistance and temperature values, with a cycle time of 5 seconds. The labview block diagram for the measurement is shown in Figure 4.7.

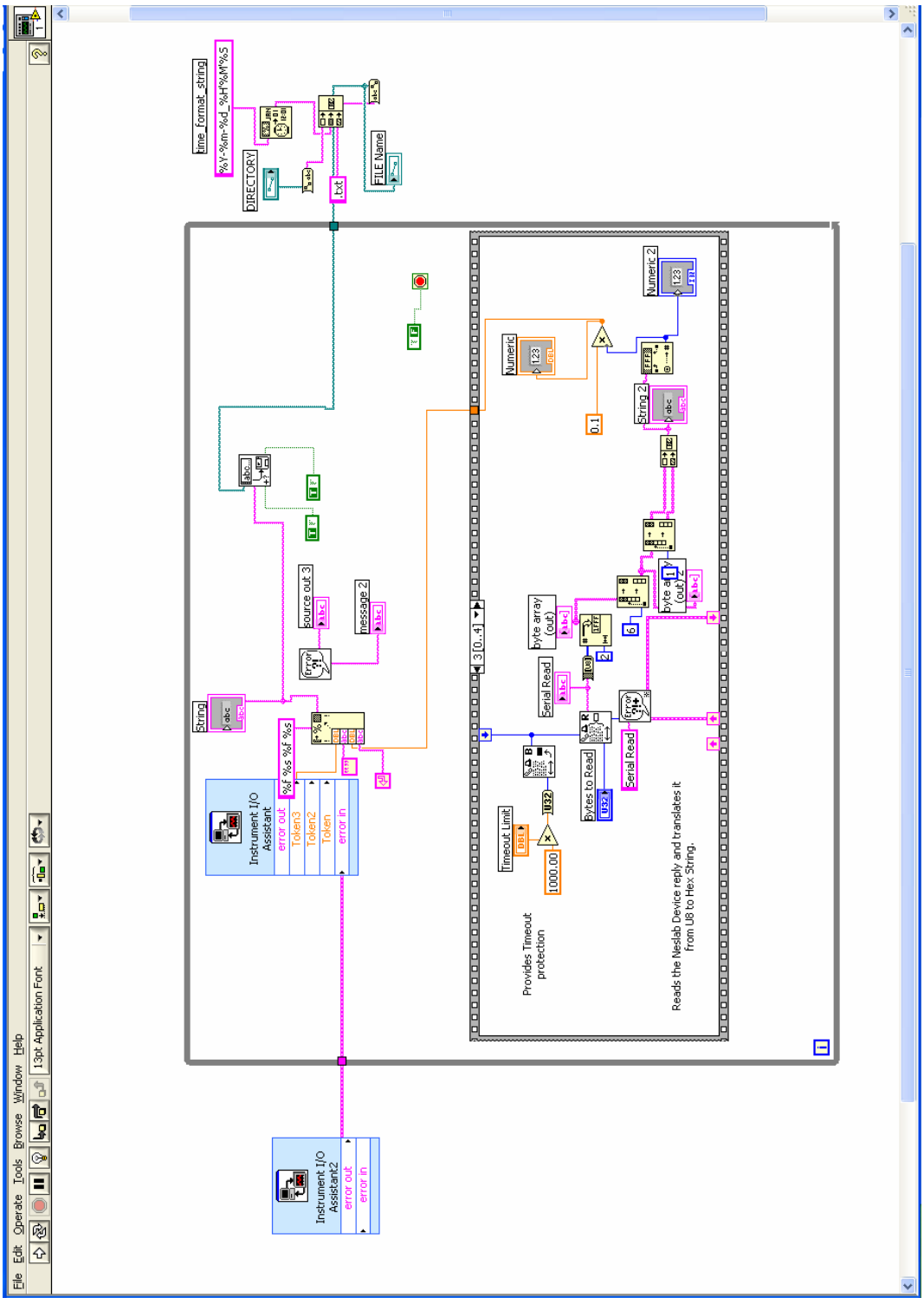

Figure 4.7 Labview block diagram

CHAPTER 5

RESULTS AND DISCUSSIONS

In this chapter the results of the fabricated temperature sensors are presented. They are categorized based on the mechanism of sensing and the processing conditions in which the sensors were fabricated. The influence of the parameters of diffusion is discussed.

5.1 Outdiffusion

The silicon surface after gold diffusion could be easily identified by the naked eye. This was due to the outdiffusion of gold to the silicon surface during the cooling period. As gold diffuses following a substitutional-interstitial mechanism, it can move to dislocations and precipitate there on cooling [22, 26]. The silicon surface acts as a source of dislocations which explains the precipitation of gold on the surface. Figure 5.1 shows the sensor and the optical image of diffused surface. When observed closely, the polished surface of the wafer is covered with high density of etch pits due to high concentrations of gold precipitates. No specific pit structure could be distinguished though. The interface of the diffused region and bare silicon is also shown.

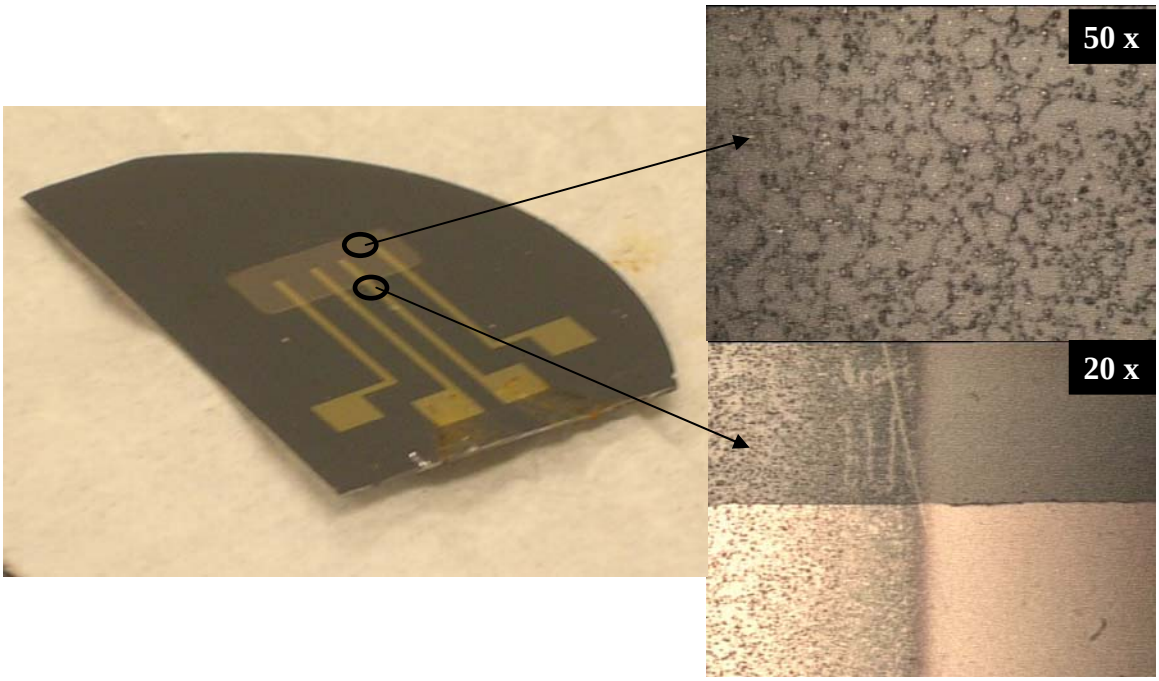

Figure 5.1 Optical image of the sensor surface

5.2 Resistivity measurements

The resistivity measurements were done using a four point probe. The resistivity of the sample is calculated using eq. 4.1, with the assumption that gold diffused throughout the wafer (depth). The influence of time of diffusion, temperature of diffusion and ambient was investigated.

5.2.1 Influence of time of diffusion

To understand the effect of time of diffusion on the resistivity of silicon, 250Å of gold was deposited on different areas of a silicon wafer. The wafer was then cut and each piece of silicon was diffused in oxygen ambient at 950˚C for times ranging from 30 minutes to 2 hours. Resistivity of the diffused regions was measured at room temperature and is tabulated in Table 5.1. It was observed that the resistivity increased proportionally

as the time of diffusion increases as expected from Fick's laws (section 3.2.1). From Figure 3.7 this can be attributed to increase in the gold concentration from 10^{14} atoms/cm^3 to 10^{15} atoms/cm^3. Since 10^{15} atoms/cm^3 is close to the limiting value of the gold concentration, at the diffusing temperature to remain an n-type silicon, the diffusion time for fabrication of the sensor was set at 2 hours.

Table 5.1 Resistivity measurements of samples diffused in oxygen ambient @ 950˚C

Time of diffusion (minutes)	Current (A)	Voltage (V)	Resistivity (Ω-cm)
30	4.53×10^{-6}	0.0576	1440
60	4.53×10^{-6}	0.46	11500
90	4.53×10^{-6}	0.81	20250
120	4.53×10^{-6}	3.0	75000

5.2.2 Influence of diffusing temperature

Gold was diffused in silicon at various temperatures. The wafers were diffused in certain regions with gold using shadow masks during deposition. The diffusion time was kept constant at 2 hours. The resistivity of the samples is tabulated in Table 5.2. It is seen that as the temperature of diffusion was increased the resistivity increased. The increase can be attributed to potentially higher and more uniform gold concentration due to enhanced diffusion constant as shown in eq. 3.3.

Table 5.2 Resistivity measurements of samples diffused at various temperatures for 2 hours

Temperature of diffusion (˚C)	Ambient	Current (A)	Voltage (V)	Resistivity (Ω-cm)
1000	O_2	4.53×10^{-6}	4.3	107500
1050	O_2	4.53×10^{-7}	1.62	405000
1100	O_2	4.53×10^{-7}	1.7	425000
1000	N_2	4.53×10^{-6}	0.38	9500
1050	N_2	4.53×10^{-6}	5.8	145000
1100	N_2	4.53×10^{-6}	8.8	220000

5.2.3 Influence of diffusing ambient

The effect of diffusion atmosphere can be inferred from Table 5.2. The samples diffused in oxygen environment have a higher resistivity value than the samples diffused in nitrogen environment.

This can be attributed to oxidation enhanced diffusion (OED) of gold in silicon. During thermal oxidation there is a supersaturation of interstitials and an undersaturation of vacancies. Hence impurities that diffuse interstitially into silicon have enhanced diffusion and impurities that diffuse due to the vacancies have retarded diffusion during thermal oxidation [27, 28].

Nitrogen suppresses the “grown-in defect” formation in silicon. This leads to a decrease in the substitutional gold concentration [29]. This is one of the possible reasons

for the resistivity of sensors diffused in nitrogen environment having a lower value as compared to the sensors diffused in oxygen environment.

5.2.4 Influence of temperature on resistivity

Figure 5.2 shows the effect of temperature on resistivity of a 20Ω-cm n-type silicon wafer. This measurement was done using a four point probe and a hot plate. It is seen that the resistivity of n-type silicon increases as the temperature is increased. The mobility and density of electrons are functions of doping concentrations. In lightly doped samples (e.g. the sample with doping of 10^{14}-10^{15} cm^{-3}), the lattice scattering dominates, and the mobility decreases as the temperature increases. Hence the resistivity increases as temperature increases.

This can be used as a temperature sensor and a similar prototype based on p-type silicon wafer has been developed by Gupta et. al. [12]. Sensitivity of such a silicon sensor is very low. Higher sensitivities can be achieved by diffusion of gold in silicon as discussed in section 3.1.

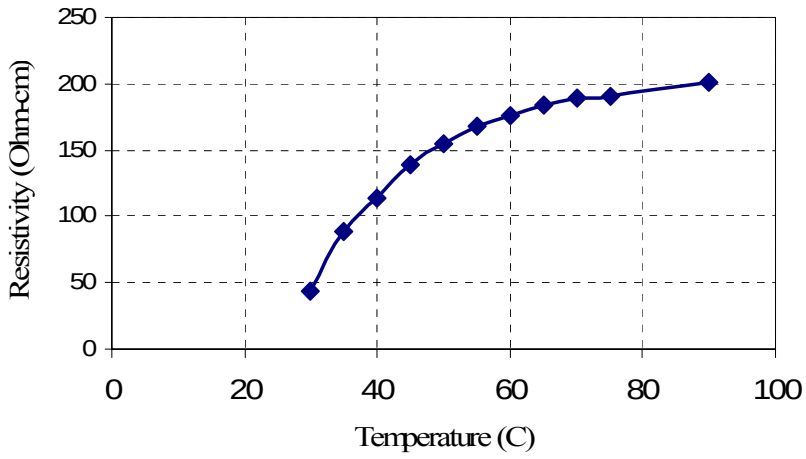

Figure 5.2 Plot of resistivity vs. temperature for n-type silicon wafer

Gold was diffused in the silicon wafer at 1050˚C in oxygen ambient for 2 hours. The effect of gold diffusion in the n-type wafer leads to an increase in resistivity due to compensation of impurities and is explained in detail in section 3.4.1. As temperature increases some electrons from valence band states are excited to the conduction band by thermal energy, leaving behind an equal number of holes in the valence band. Hence the TCR changes from positive for lightly doped samples, to negative after gold diffusion and the resistivity decreases as temperature increases as is shown in Figure 5.3.

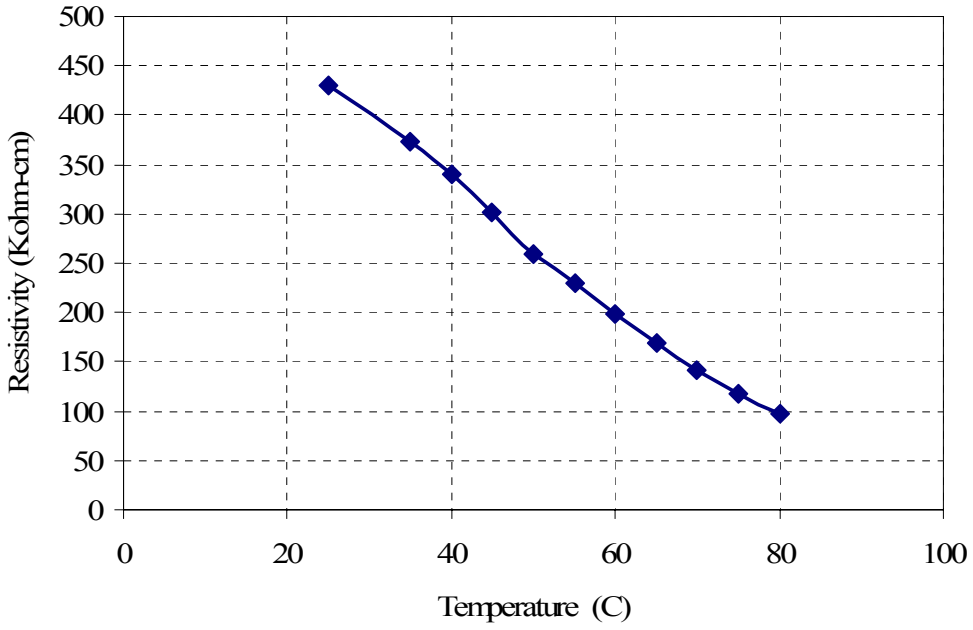

Figure 5.3 Plot for resistivity vs. temperature plot for n-type silicon wafer with gold diffused @ 1050 ˚C

It is seen that the resistivity of silicon increases from 10-20Ω-cm to around 400KΩ-cm at room temperature. This data can be used to infer the concentration of gold in silicon by referring to Figure 3.7. The maximum solubility of gold in silicon is 10^{15}

atoms/cm^3 [22]. It can be seen that for a phosphorus concentration of 2x10^{14} the resistivity reaches 400KΩ-cm when the gold concentration is around 10^{15} atoms/cm^3.

5.3 Resistance measurements

The resistance measurements were done using a temperature bath and a multimeter interfaced using labview as discussed in section 4.3. Figures 5.4 – 5.9 show the response of sensors fabricated in both oxygen and nitrogen ambient at 1050˚C for 2 hours.

The responses of the sensors were fit with model curves. The curve fitting models were considered a good fit if they were 98% accurate. R^2 is a statistical value that represents how closely the curve fit matches the data points**.** The dashed curves in the Figures represent the fitting models.

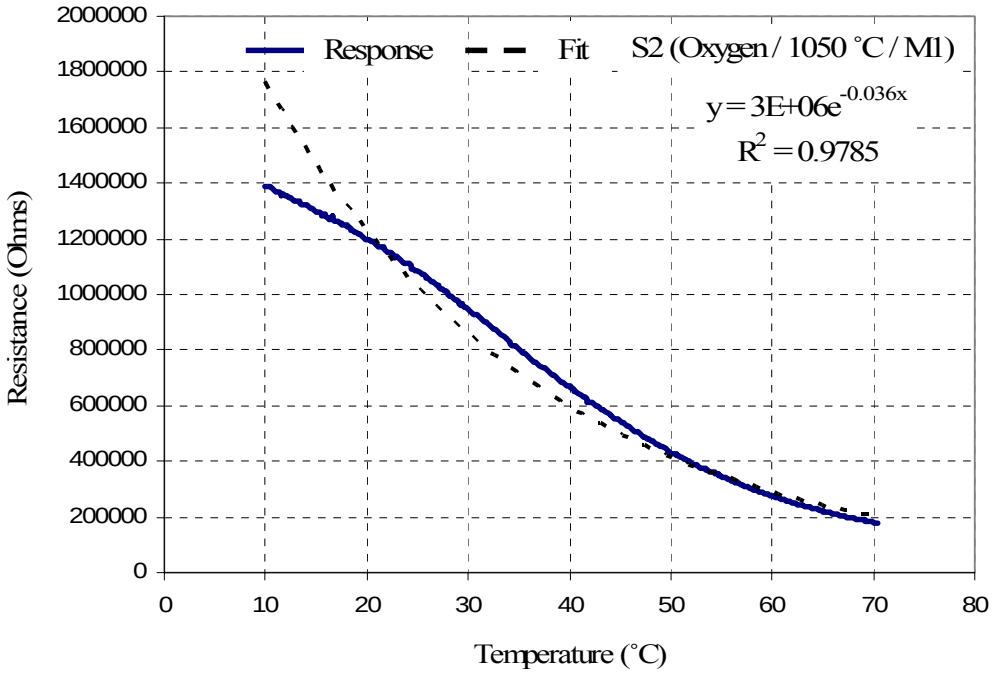

Figure 5.4 Response of sensor fabricated @ 1050˚C in oxygen environment (M1)

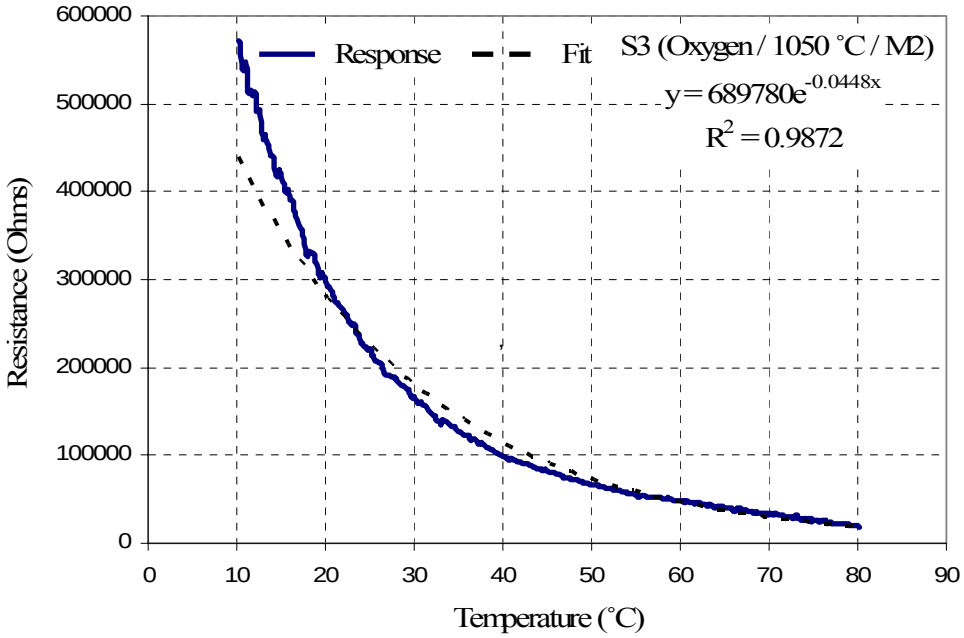

Figure 5.5 Response of sensor fabricated @ 1050 ˚C in oxygen environment (M2)

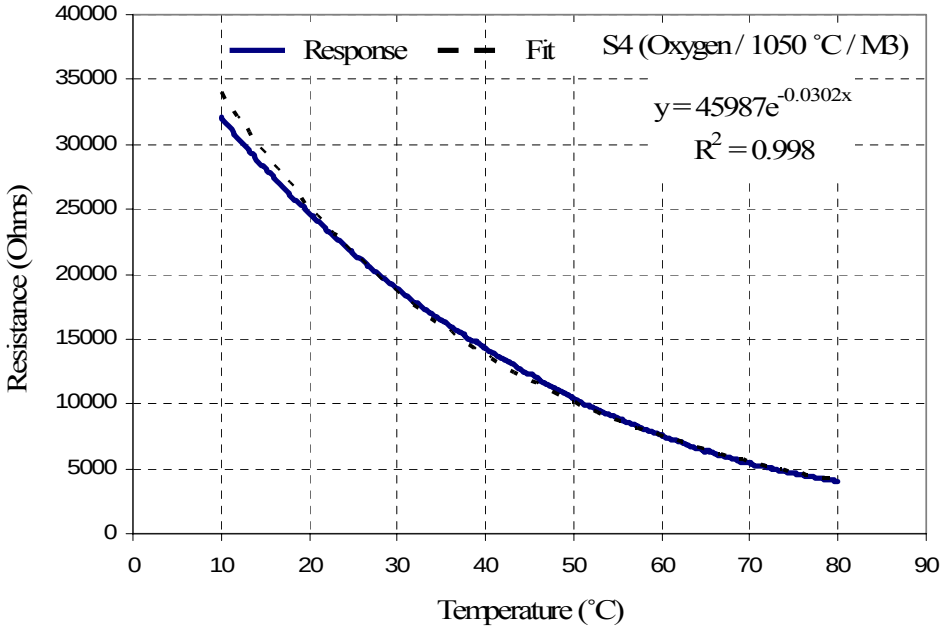

Figure 5.6 Response of sensor fabricated @ 1050 ˚C in oxygen environment (M3)

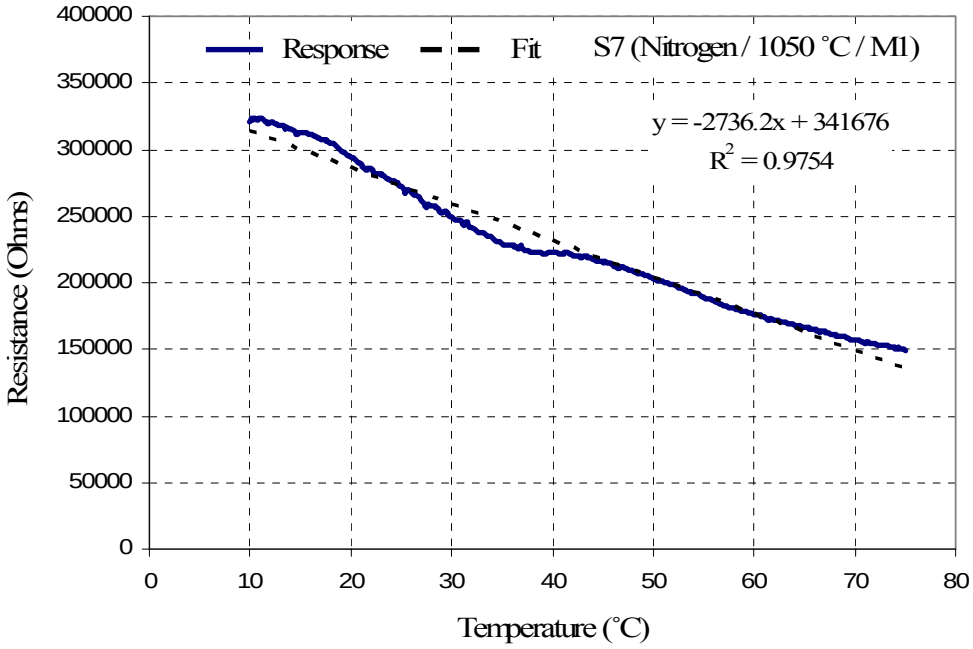

Figure 5.7 Response of sensor fabricated @ 1050 ˚C in nitrogen environment (M1)

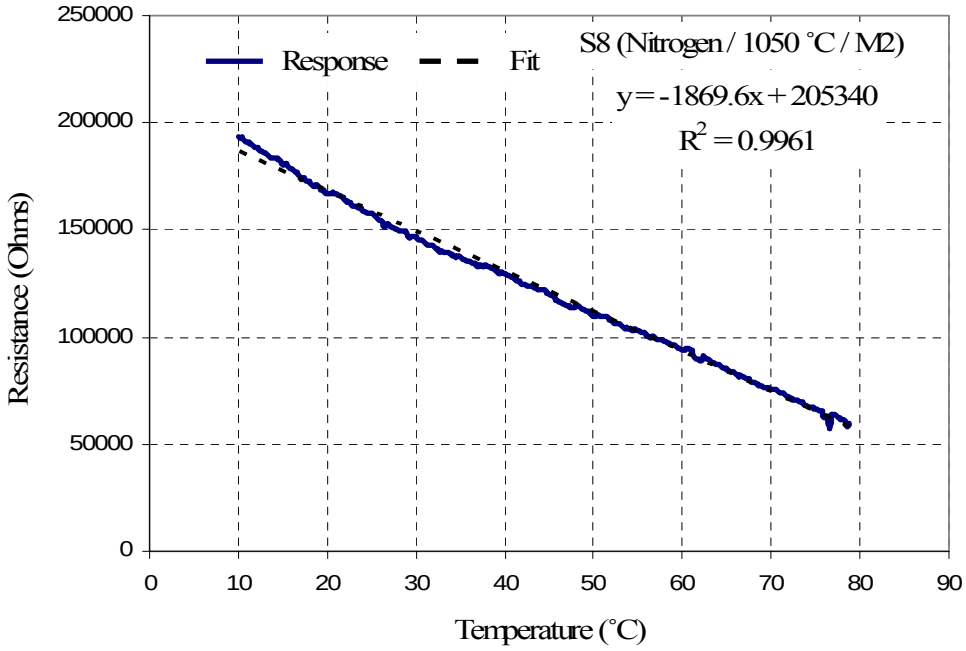

Figure 5.8 Response of sensor fabricated @ 1050 ˚C in nitrogen environment (M2)

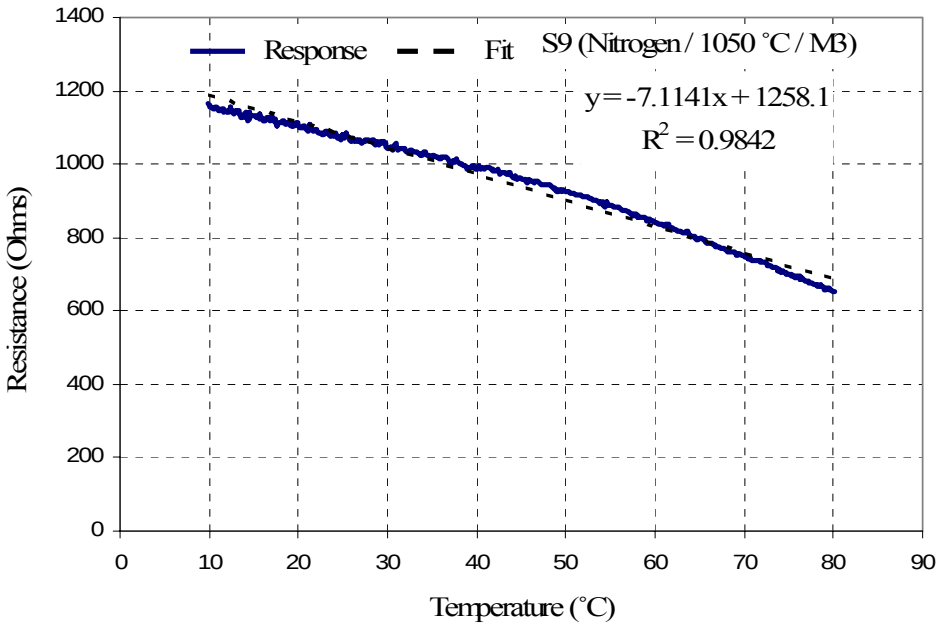

Figure 5.9 Response of sensor fabricated @ 1050˚C in nitrogen environment (M3)

A noticeable change in resistance was observed for a 0.1˚C change in temperature. Hence the resolution of the sensor can be safely assumed as 0.1˚C. The change in temperature of 0.1˚C is limited by the testing equipment capability.

5.3.1 Influence of ambient

It is seen that the sensors fabricated in an oxygen environment have higher resistance values as compared to the sensors fabricated in nitrogen environment. This is due to the OED of gold in silicon and suppression of gold concentration when diffused in nitrogen as discussed earlier. The responses of sensors fabricated in oxygen environment were found to have an exponential fit. As shown in Figure 3.8 the resistivity variation with temperature of silicon diffused with gold in oxygen environment followed a log-

linear trend. The sensors fabricated in nitrogen a linear fit. No explanation or data has been documented for this behavior.

5.3.2 Influence of diffusing area

It is observed that the resistance value of the sensor changes with the diffused area. Sensors fabricated with dimension M1 (10mm x 5mm) were found to have the highest resistance value for both the oxygen and the nitrogen ambient. These were followed by M2 (10mm x 2mm) and M3 (5mm x 2mm). The resistance value hence was directly proportional to the area of diffusion. This can be attributed to the lateral diffusion phenomena. It was observed that the resistivity of the silicon wafer around the diffused region also changed dramatically due to the lateral diffusion of gold. Hence in larger areas more gold concentration is present at the center of the sample and hence a larger resistance value.

5.3.3 Influence of diffusing temperature

Sensors were fabricated by diffusing gold into a fixed area of silicon at temperatures ranging from 1000˚C to 1100˚C. The influence of temperature of diffusion is shown in Figure 5.10 and Figure 5.11.

The wafers diffused at higher temperature have higher resistance values in the case of both the oxygen and nitrogen ambient. This can be attributed to higher temperatures leading to more gold diffusion in silicon and hence higher resistivity.

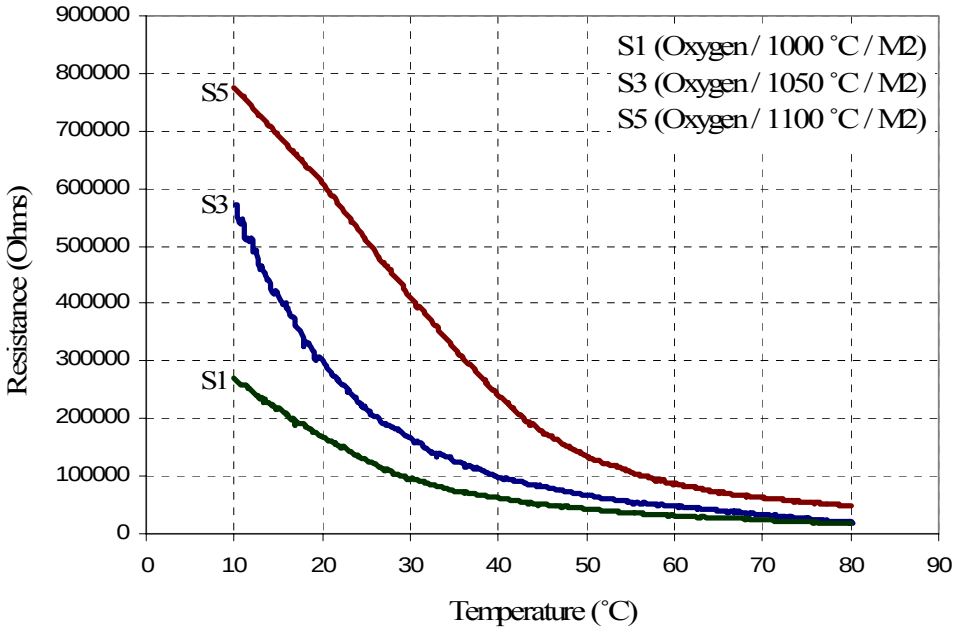

Figure 5.10 Comparison of sensors fabricated in oxygen environment at different temperatures (M2)

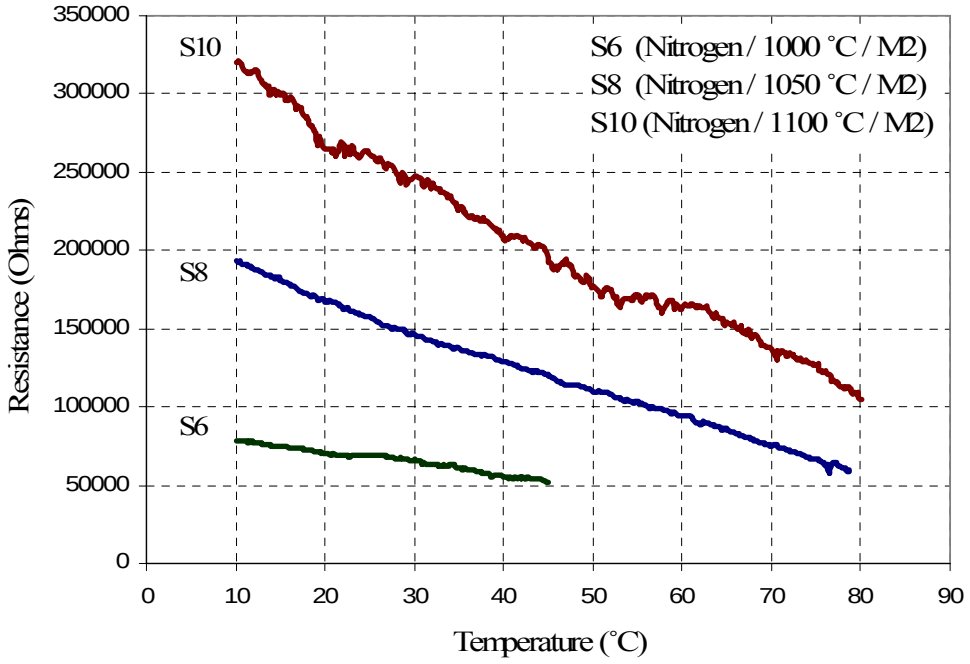

Figure 5.11 Comparison of sensors fabricated in nitrogen environment at different temperatures (M2)

5.4 Performance criteria

The performance criteria of the sensors that were evaluated were sensitivity, hysteresis and noise.

5.4.1 Sensitivity

The *sensitivity* of the fabricated sensors is defined as the amount of change in resistance for an increment of 1˚C in temperature. In Tables 5.3 – 5.4 the results of the fabricated sensors are presented. The sensitivity of the sensors is inferred from the respective curve fits.

Table 5.3 summarizes the sensors that were fabricated in oxygen environment. The equations for the exponential fit are tabulated and the accuracy of the fit is also shown. It is not possible to have a single sensitivity value for an exponential response and is not tabulated.

Table 5.3 Response of sensors fabricated in oxygen environment

Sample	Diffusion Parameters (Ambient/˚C/Mask)	Exponential Equation R=f(T)	Accuracy (%)
S1	O_2 / 1000 / M2	$R = 332364e^{-0.0387.T}$	98.24
S2	O_2 / 1050 / M1	$R = 3E+06e^{-0.0360.T}$	97.85
S3	O_2 / 1050 / M2	$R = 689780e^{-0.0448.T}$	98.72
S4	O_2 / 1050 / M3	$R = 45987e^{-0.0302.T}$	99.8
S5	O_2 / 1100 / M2	$R = 1E+06e^{-0.0446.T}$	98.96

Table 5.4 presents the results of sensors fabricated in nitrogen environment. The sensitivity of the sensors is also tabulated. It is seen that the sensitivity is directly proportional to temperature and the area of diffusion.

Table 5.4 Response of sensors fabricated in nitrogen environment

Sample	Diffusion Parameters (Ambient/˚C/Mask)	Linear Equation R=f(T)	Accuracy (%)	Sensitivity (Ω/˚C)
S6	N_2 / 1000 / M2	R = -733.93T + 86220	97.98	733.9300
S7	N_2 / 1050 / M1	R = -2736.2T + 341676	97.54	2736.2000
S8	N_2 / 1050 / M2	R = -1869.6T + 205340	99.61	1869.6000
S9	N_2 / 1050 / M3	R = -7.1141T + 1258.1	98.42	7.1141
S10	N_2 / 1100 / M2	R = -2832.3T + 331694	98.33	2832.3000

5.4.2 Hysteresis

Hysteresis is defined as the phenomenon in which the response of a physical system to an external influence depends not only on the present magnitude of that influence but also on the previous history of the system. The sensors were tested for hysteresis by testing for many cycles of temperature changes. Each cycle consisted of ramping up and down of temperature. Figure 5.12 shows the response of sample S2 (O_2 / 1050 ˚C / M1) to two temperature cycles. Hysteresis occurs between the heating and the cooling parts of the cycle and between various cycles. Hysteresis can be eliminated by having better material characterization or using signal conditioning electronic circuitry.

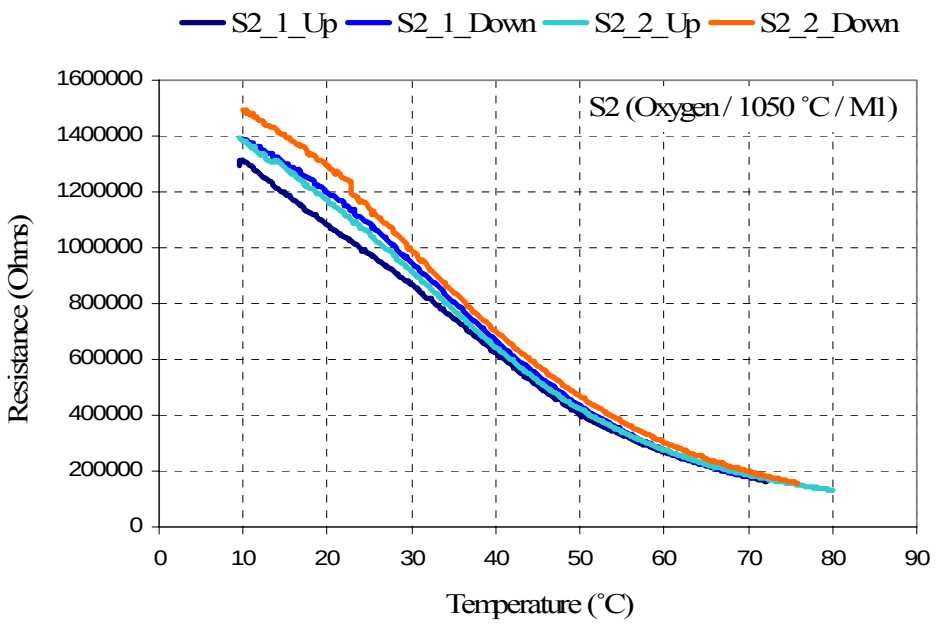

Figure 5.12 Hysteresis response of fabricated sensor

5.4.3 Noise

Noise is described as the positive and negative fluctuations about an unchanging (over a long time scale) average value. In order to determine the noise, the sensor was maintained at a constant temperature of 20˚C for 45 minutes and the resistance changes were logged on. The sensor response was within ±1% of the average value as seen from Figure5.13.

This behavior can also be attributed to the feedback control loop of the temperature bath. The observed resistance changes are probably due to the variations in temperature occurring due to the circuitry of the bath, and not necessarily noise in the system.

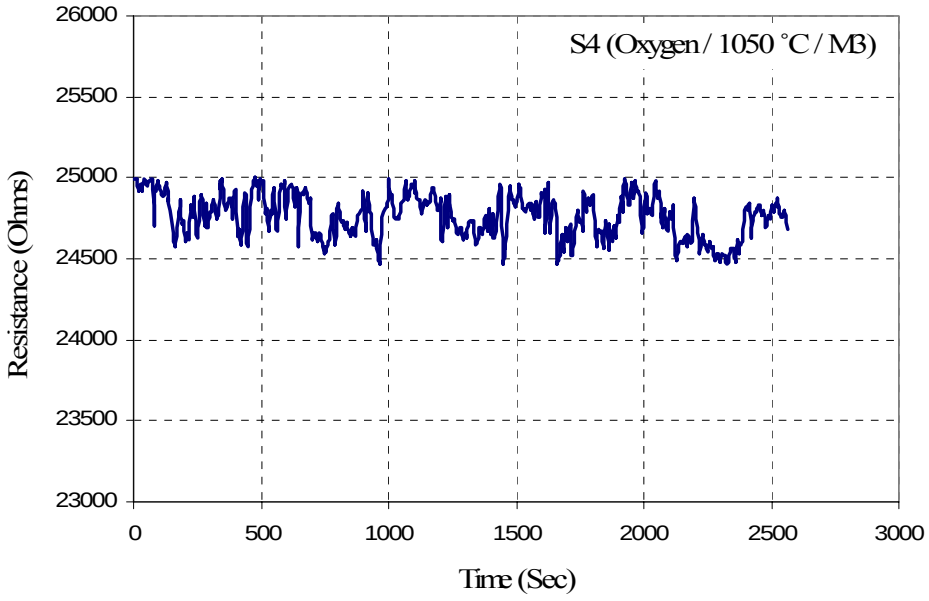

Figure 5.13 Response of a sensor at a constant temperature of 20°C

CHAPTER 6

CONCLUSIONS AND FUTURE WORK

6.1 Conclusions

In this work bulk silicon based temperature sensors were fabricated by altering the electrical properties of silicon using gold diffusion. Gold is diffused into silicon at temperatures ranging from 1000˚C to 1100˚C for 2 hours in both oxygen and nitrogen environments. It is shown that the environment in which gold is diffused is very critical for the fabrication of the sensors. Also the size of the diffused region affects the performance of the sensor. Sensors for different applications can be fabricated by altering the diffusing environment. The fabricated sensors are highly sensitive and are capable to measure small temperature changes.

The sensors fabricated in oxygen environment have an exponential response and hence the sensitivity is not calculated, but the change in resistance is very high for a minimal change in temperature. The sensors fabricated in nitrogen environment have a linear response and have sensitivity ranging from 7Ω/˚C to 3000Ω/˚C which is better than any reported resistive bulk silicon based temperature sensor. The sensors have a resolution of at least 0.1˚C as it is the limitation of the testing setup, but the resistance change observed for 0.1˚C suggests that the sensors are capable to measure much lower temperature changes.

Commercial sensors are available that can be operated in the particular temperature ranges. SE95 by Philips semiconductors is an IC based temperature sensor with an operating range from -25˚C to 100˚C with a resolution of 0.125˚C. A commercial CTD sensor Seabird 911 has a temperature sensor with the operating range -5˚C to 35˚C with a resolution of 0.0002˚C but costs in the range of $2000. The sensor fabricated in this work has high resolution and can be manufactured very cheaply.

6.2 Implementation strategy

The wafers diffused in oxygen environment have much higher resistance than the wafers diffused in nitrogen environment. This leads to different sensitivity for samples that were diffused in oxygen environment as compared to the nitrogen environment.

It is observed that the response of samples that were diffused in the oxygen environment have an exponential response and the samples diffused in the nitrogen environment have a linear response. As discussed in earlier chapters, the two applications that the present work is targeted to are the CTD sensor and magnetocaloric microcoolers. The temperatures that need to be measured in ocean range from 35˚C to 0˚C and -20˚C to 20˚C for the targeted microcooler application.

The sensors fabricated in nitrogen environment suggest that they can be used for both the data ranges. The sensors fabricated in the oxygen environment can be used in the CTD sensor as they can provide more sensitivity than the sensors fabricated in the nitrogen environment in that temperature range. The response suggests that it would not be easy to measure sub-zero temperatures, by samples diffused in oxygen ambient, as the resistance will be too high in those temperature ranges. The responses of samples

diffused in nitrogen environment suggest measurable resistance values in sub-zero temperatures and can be used for the microcooler application.

It is also seen that the temperature and area of diffusion affects the resistance values and the type of response. It would be possible to tailor the response of the sensor to fit a particular range of values by altering the dimensions of diffused area and the diffusion environment.

6.3 Future work

A more calibrated test setup with temperature changes in the range of 0.01˚C or lower can be used to get more accurate measurements. Smaller dimensions for gold diffusion can be attempted to make this a genuine MEMS sensor. Hysteresis can be removed by using signal conditioning circuits. The effect of the temperature bath on the noise in the sensor can be tested. A higher resolution temperature sensor can be used as reference for the calibration of the noise. As the sensor needs to be under-water for the CTD application the effect of pressure on the sensor has to be investigated.

More study is required to understand the physics of gold diffusion in silicon. This will help to understand better the parameters that critically effect the diffusion which will help in controlling the thermal diffusion better. Also the effect of orientation of wafers on diffusion can be studied. Ion-implantation of gold can be attempted, and its effect on resistivity investigated. Ion-implantation has the advantage of minimal lateral diffusion and hence would be very easy for fabricating an integrated temperature sensor on a silicon chip that will have many sensors/devices eventually, without it affecting the performance of other sensors/devices.

REFERENCES

[1] **http://www.seabird.com/products/spec_sheets/911data.htm**, Sea-Bird Electronics, Oct. 2005

[2] S. Aravamudhan, S. Bhat, B. Bethala, S. Bhansali, L. Langebrake, " MEMS based integrated conductivity-temperature-depth (CTD) sensor for harsh oceanic environment", *IEEE Oceans*, Washington D. C., September 19 – 23, 2005

[3] S. C. Kim, B. Bethala, S. Ghirlanda, S. Sambandam, S. Bhansali, " Design and fabrication of a magnetocaloric microcooler", *ASME International Mechanical Engineering Congress and Exposition*, 2005

[4] http://www.capgo.com/Resources/InterestStories/TempHistory/TempHistory.html Capgo Pty Ltd, Oct. 2005

[5] L. Michalsky, K. Eckersdorf and J. McGhee, "Temperature Measurement", Wiley Publications, 2001

[6] J. Shieh, J.E. Huber, N.A. Fleck and M.F. Ashby, "The selection of sensors", *Progress in Mater. Sci.*, 2001, Vol. 46, pp. 461 – 504

[7] G. C. M. Meijer and A.W. Herwaarden, "Thermal Sensors", IOP Publishing, 1994

[8] http://www.wici.com/technical_info/articles/temp_prm/tmprmch1.htm, Wilkerson Instrument Co. Inc., Oct 2005

[9] J. -J. Park and M. Taya, "Micro-temperature sensor array with thin-film thermocouples", *Electronics Letters*, 13th May 2004, Vol. 40, No. 10, pp. 599 – 601

[10] V. F. Mitin, V.V. Kholevchuk and R.V. Konakova, "Temperature microsensors", *IEEE Semicond. Conf.*, Oct. 1999, Vol. 2, pp. 495 – 498

[11] K. S. Sazda, C. G. Sodini and H. F. Bowman, "A low noise, high resolution silicon temperature sensor", *IEEE Journal of Solid State Circuits*, 1996, Vol. 31, No. 9, pp. 1308 - 1313

[12] R. Gupta and G. Bose, "Design and fabrication of bulk silicon based temperature sensor", *J. Indian Inst. Sci.*, Sept. – Oct. 2001, 81, pp. 557-561

[13] H. J. Qiu and G. J. Maclay, "Investigation of a low-cost broad range silicon based temperature sensor", *IEEE Trans. on Industry Appl.*, Sept. – Oct. 1999, Vol. 35, No. 5, pp.1178 -1183

[14] A. K. Kewell, G. T. Reed and F. Namavar, "Integrated temperature sensor in Er-doped silicon", *Sensors and Actuators A*, 65, 1998, pp. 160 - 164

[15] S. K. Gamage, N. Okulan and H. T. Henderson, "Behavior of bulk micromachined silicon flow sensor in the negative differential resistance regime", *J. Micromech. Microeng.*, 2000, pp. 421 - 429

[16] D. Shaw, "Atomic Diffusion in Semiconductors", Plenum press, 1973

[17] L.V. Zhigilei, http://www.people.virginia.edu/~lz2n/mse209/Chapter5.pdf , *Introduction to Material Science*, Oct. 2005

[18] R. M .Burger and R. P. Donovan, "Fundamentals of silicon integrated device technology", Prentice Hall, 1967

[19] K. Malik, R. J. Falster and P. R. Wilshaw, "'Semi-insulating' silicon using deep level impurity doping: problems and potential", *Semicond. Sci. Technol.*, 2003, 18, pp. 517 - 524

[20] A. G. Milnes, "Deep impurities in semiconductors", Wiley Publication, 1973

[21] U. M. Gösele, "Fast diffusion in semiconductors", *Ann. Rev. Mater. Sci.*, 1988, 18, pp. 257 – 282

[22] W. M. Bullis, "Properties of gold in silicon", *Solid State Electronics*, 1966, Vol. 9, pp. 143 – 168

[23] C. B. Collins, R. O. Carlson and C. J. Gallagher, "Properties of gold-doped silicon", *Phys. Rev.*, 1957, Vol. 105, No. 4, pp. 1168 – 1173

[24] D. Mathiot, "Gold, self-, and dopant diffusion in silicon", *Phys. Rev. B*, 1992, Vol. 45, No.23, pp. 13345 – 13355

[25] R. C. Jaeger, "Introduction to microelectronic fabrication", Prentice Hall, 2002

[26] K. Graff, "Metal impurities in silicon-device fabrication", Springer Series, 2000

[27] L. S. Adam, “Experimental investigation of transient enhanced diffusion of phosphorus in silicon in the MeV range”, Master’s Thesis, UF, 1997

[28] S. M. HU, “Formation of stacking faults and enhanced diffusion in the oxidation of silicon”, *J. of Appl. Phys.*, 1974, Vol. 45, No. 4, pp.1567 – 1573

[29] A. L. Parakhonsky, E. B. Yakimov and D. Yang, “Nitrogen effect on gold diffusion in Cz Si”, *Physica B*, 2001, pp. 396 - 399